Human Cochlea: Anatomical Characteristics and Their Relevance for Cochlear Implantation

HELGE RASK-ANDERSEN,[1]* WEI LIU,[1] ELSA ERIXON,[1] ANDERS KINNEFORS,[1]
KRISTIAN PFALLER,[3] ANNELIES SCHROTT-FISCHER,[2]
AND RUDOLF GLUECKERT[2]

[1]Department of Otolaryngology, Uppsala University Hospital, 75185 Uppsala, Sweden
[2]Department of Otolaryngology, Medical University of Innsbruck, 6020 Innsbruck,
Anichstraße 35, Austria
[3]Division of Histology and Embryology, Innsbruck Medical University, Innsbruck, Austria

ABSTRACT

This is a review of the anatomical characteristics of human cochlea and the importance of variations in this anatomy to the process of cochlear implantation (CI). Studies of the human cochlea are essential to better comprehend the physiology and pathology of man's hearing. The human cochlea is difficult to explore due to its vulnerability and bordering capsule. Inner ear tissue undergoes quick autolytic changes making investigations of autopsy material difficult, even though excellent results have been presented over time. Important issues today are novel inner ear therapies including CI and new approaches for inner ear pharmacological treatments. Inner ear surgery is now a reality, and technical advancements in the design of electrode arrays and surgical approaches allow preservation of remaining structure/function in most cases. Surgeons should aim to conserve cochlear structures for future potential stem cell and gene therapies. Renewal interest of round window approaches necessitates further acquaintance of this complex anatomy and its variations. Rough cochleostomy drilling at the intricate "hook" region can generate intracochlear bone-dust-inducing fibrosis and new bone formation, which could negatively influence auditory nerve responses at a later time point. Here, we present macro- and microanatomic investigations of the human cochlea viewing the extensive anatomic variations that influence electrode insertion. In addition, electron microscopic (TEM and SEM) and immunohistochemical results, based on specimens removed at surgeries for life-threatening petroclival meningioma and some well-preserved postmortal tissues, are displayed. These give us new information about structure as well as protein and molecular expression in man. Our aim was not to formulate a complete description of the complex human anatomy but to focus on aspects clinically relevant for electric stimulation, predominantly, the sensory targets, and how surgical atraumaticity best could be reached. Anat Rec, 00:000–000, 2012. ©2012 Wiley Periodicals, Inc.

Key words: human cochlea; anatomical variations; ultrastructure; cochlear implantation; trauma
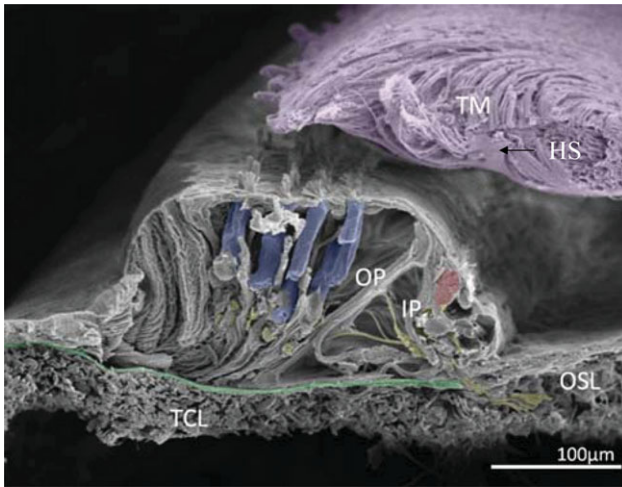
Fig. 1. Scanning electron micrograph (SEM) of the organ of Corti (OC) in a human cochlea that was sacrificed due to surgery for life-threatening petroclival meningioma. Patient's hearing was normal, and ethical/patient consents were obtained.* Tonotopic region approximates the frequency region of 250–500 Hz. OC in this region contains four rows of outer hair cells (OHCs—blue). The inner pillar cell has partly collapsed. The tympanic covering layer (TCL) of the basilar membrane (BM—green) can be seen. Note the fibrous character of the tectorial membrane. HS, Hensen's stripe; inner hair cell (red); IP, Inner pillar; OP, outer pillar; OSL, osseous spiral lamina; TM, tectorial membrane; neurons; yellow.

[*Harvesting of tissue: Human inner ear specimens, without any known hearing impairment, were obtained at surgery for the removal of life-threatening large petroclival meningiomas compressing the brainstem (Tylstedt et al., 1997). The study conforms to The Declaration of Helsinki and was approved by the medical ethical committee at the Uppsala University Hospital (no. C254/4, C45/7 2007). Patient's consent was obtained.]

Human cochlea was initially described by Eustachi in 1564 and first published by Albini in Leyden in 1744. Later, the Neapolitan anatomist Cotugno (1761) described the human inner ear and cochlear anatomy using corrosion casts in *De aqueductibus Auris Humana Interna*. Ninety years later, Corti (1851) discovered the receptor organ named after him. In a monumental work, Retzius (1884) improved histologic techniques and presented meticulous descriptions of the cellular anatomy of the human cochlea including surface preparations.

For fine-structure analyses of the human cochlea, good fixation is critical (Wright, 1980b; Gleeson, 1985; Osborne et al., 1989; Comis et al., 1990). In earlier studies, most human inner ears have been studied using perilymphatic fixation some hours after death (Bredberg, 1968; Bredberg et al., 1970). Several studies were performed on mammalian cochlea using SEM, but only a few on the human cochlea (Lim and Lane, 1969; Lim, 1972; Hunter-Duvar, 1975; Hoshino, 1977; Nomura and Kawabata, 1979; Wright, 1980b, 1981a,b, 1982, 1983; Nadol, 1983; Nadol and Burgess 1994; Bagger-Sjöbäck and Engström, 1985; Gleeson, 1985; Engström et al., 1987, 1990; Osborne et al., 1989; Comis et al., 1990; Hoshino, 1990; Reiss, 1990; Reiss and Vollrath, 1990; Pujol et al., 1991). Some were assessed in embryos (Tanaka et al., 1979; Igarashi, 1980; Fujimoto et al., 1981; Hoshino and Nakamura, 1985; Lavigne-Rebillard et al., 1985a,b; Lavigne-Rebillard and Pujol, 1986, 1987;

Hoshino, 1990; Pujol et al., 1991). Here, we present results from ultrastructural analyses of human inner ear specimens obtained at surgery (Fig. 1). Swift fixation can be executed in the operating room to improve cell preservation. Bone minerals were removed with 10% Na-EDTA. Besides, it is possible to carry out immunohistochemistry with confocal microscopy for detailed protein detection. The surgical technique was described earlier (Tylstedt et al., 1997). Tissue can be regarded as "near-normal," because the tumor extension does not involve the cochlea and audiometry displayed normal age-related tone thresholds. However, drilling could cause some damage, and structural/physiological changes might occur in middle-aged individuals despite normal hearing. Results show some discrepancies in anatomical structure and protein expression between rodents and man highlighting that *men are not simply big mice*.

A particularly important clinical issue is the slow retrograde degeneration of human auditory neurons following hair cell loss. This has immense significance and makes the cochlear implantation (CI) technique achievable over time. Experience suggests that functional neurons may remain; a blessing for the CI patient. The reason for this may reside in factors protecting the neurons such as neural architecture, neuron interaction, secreted protectants, or simply the inborn biological turn over or life span. However, these factors are important to explore. We do not yet recognize if electric stimulation may exert neurotrophic effects on human auditory neurons or influence their survival. Moreover, experimental models diverge here. Some studies in animals have demonstrated survival effects with electrical stimulation (Lousteau, 1987; Hartshorn et al., 1991; Leake et al., 1991, 1995, 1999; Miller et al., 1995; Mitchell et al., 1997; Kanzaki et al., 2002), while other studies report no rescue of SGNs associated with electrical stimulation (Shepherd et al., 1994, 2005; Araki et al., 1998; Li et al., 1999; Coco et al., 2006; Agterberg et al., 2010). A temporal bone study of 11 cochlear implant patients' temporal bones showed no evidence of enhanced neuron survival in the implanted ear compared to the unimplanted ear (Khan et al., 2005).

HUMAN COCHLEA—GROSS MORPHOLOGY

The two human cochleae are mirror-shaped, fluid-filled, coiled, fairly symmetrical bony tubes (3.2–4.2 cm long) situated in the petrous pyramids of the temporal bones. Perilymph; the fluid inside the scalae vestibuli and tympani communicates with the CSF via the cochlear aqueduct (Fig. 2). This route of fluid communication can allow spread of infections between these fluid compartments. The human cochlea is composed of ~2 and three-fourth turns (Hardy, 1938), but unusual anatomy with cochlear three turns has been described (Tian et al., 2006). It is surrounded by a compact bony structure; the otic capsule. It is the hardest bone in the body with a trilamellar arrangement with islands of modified cartilage and high-mineral content, which increases the stiffness of the bony labyrinth (Bast, 1942). This is desirable, so that vibrations of fluid in the cochlea are reflected and not absorbed by the temporal bone. At dissection (Fig. 2), the otic capsule contrasts in yellow color to that of the surrounding cortical bone.
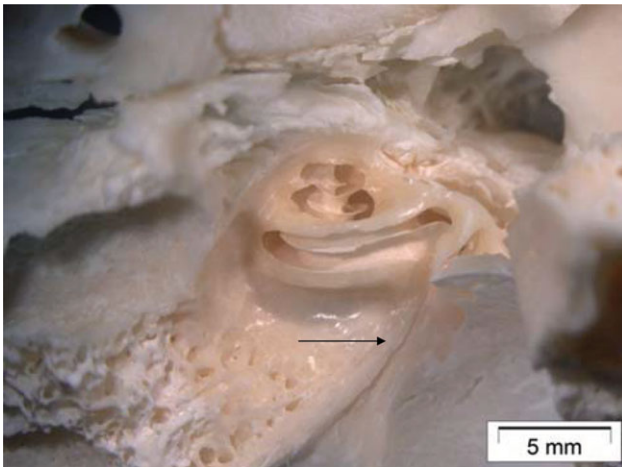
Fig. 2. Microdissection of a left side human cochlea. The otic bone is yellow. Normally, three turns are present. The cochlear aqueduct (arrow) is seen as a triangularly shaped bony channel connecting scala tympani with the subarachnoid space (Rask-Andersen et al., 1977).

There is now much focus on cochlear anatomy due to surgical approaches to electrically stimulate the auditory nerve. Studies of plastic corrosion casts, made from unselected temporal bones harvested at autopsy (Wilbrand et al., 1974, Wadin, 1988), show the extensive anatomic variations in dimension, form, and shape (Dimopoulos and Muren, 1990; Erixon et al., 2009; Rask-Andersen et al., 2010) (Figs. 3–5). Also, the results from histologic reconstruction measuring the organ of Corti length demonstrate these variations (Hardy, 1938). Hardy found that the length of the Corti organ can vary as much as 10 mm. Interesting is the high degree of bilateral symmetry, something that characterizes paired organs in the body. Surgically, the basal end of the cochlea is of great interest. It curves in three dimensions (ant.-post./lateral-medial/inf.-sup.), resembling a "fish hook." Here, a cochleostomy is made, and it is the site of the round window (RW). The hook anatomy varies which makes it difficult for the surgeon to optimally place the cochleostomy and reach scala tympani (ST) without destroying any inner ear structures.

Narrowing and remarkable coiling of the cochlea can occur that influences electrode array insertion even in normal cochleae, especially when using longer electrodes. The outer cochlear wall had a mean length of 42.0 mm (Table 1), while the first turn was 22.6 mm (range, 20.3–24.3 mm) representing 53% of the total length. Because the apical turn is small, full insertion of electrode array is hardly achievable, at least not with today's techniques. Such a deep insertion is hardly needed (and may not be advantageous), because the human spiral ganglion extends only 1 and three-fourth turns (i.e., 630°). The initiation site of the APs is not identified with certainty but may be the ganglion-cell soma in the modiolus as well as Ranvier nodes in the peripheral or central axons depending mainly on electrode position (Rattay et al., 2001a,b). Selective ion channels are now being analyzed at our laboratories.

New imaging techniques such as CT with 3D volume-rendered reconstructions can give thorough assessments of the coiling pattern; size and orientation of the cochlea relative to the skull base (Martinez-Monedero et al., 2011). This is of value before CI surgery especially in patients with malformations. Internal dimensions of the cochlear scalae and cochlear morphology related to CI were presented by Kawano et al. (1996), Verbist et al. (2009), and Biedron et al. (2010). The new technique called "cone-beam CT" improves even further image resolution and gives detailed information of the minor details of the temporal bone that is useful in CI.

Clinical Implications of Anatomic Variations

The large variations in cochlear lengths, angles between turns, and position in the skull base can influence the straightforwardness for the insertion of a CI electrode particularly passing the first turn. Most frequently damaged are the spiral ligament at the junction of the first and second half of the first turn, basilar membrane (BM), and osseous spiral lamina (Kennedy, 1987). Underdeveloped cochleae may show greater differences in the angle between the first and second turns and a smaller length of the base of the cochlea as evaluated from CT (Martinez-Monedero et al., 2011). A sharp bend of cochlear coiling in this region may hamper electrode insertion at this site. It increases the risk for perforations of cochlea membranes when the electrode tip moves from the first to the second turn. Interestingly, authors have also found that the cochlea may change its orientation during the first years of life that may require a modification of the opening of the facial recess (Lloyd et al., 2010; Martinez-Monedero et al., 2011).

HUMAN RW ANATOMY

"This is a plea of a practicing otologist rather than an experimental scientist for a re-evaluation of the round window. The writer feels that it is in this region that much future progress in intratympanic surgery will occur" (from Sellers, 1961)"

Today, there is more interest to save residual hearing when performing CI surgery, and the utility of a cochleostomy has now been questioned by several authors. Many surgeons therefore use the RW insertion technique again. This is possible through the design of new atraumatic electrode arrays. The round window membrane (RWM) is located at the end of the ST where the hook bends posteromedially. From the exterior, it is located under a bony overhang (tegmen) formed by the promontory wall of the cochlea. It is hardly seen by the surgeon due to the niche and mucosal fold. Initially, the technique used to insert a cochlear implant was through the RW. This was later abandoned for the drilling of a cochleostomy to enter the ST (Michelson, 1971; House and Urban, 1973; Clark, 1975, 1979; Burian et al., 1981). Because of the modiolus being in the way and the crista fenestra when using the RW approach, it was considered better to make a cochleostomy a few millimeters in front of the RWM (Clark et al. 1979) for the positioning of the electrode along the outer wall. Fig. 6a,b shows where surgeons may choose to drill a cochleostomy.

RWM was described by Scarpa (1747–1832) in 1772. He gave credit to Gabriele Fallopius (1523–1562) for discovering the RWM and Fabricius de Aquopendente
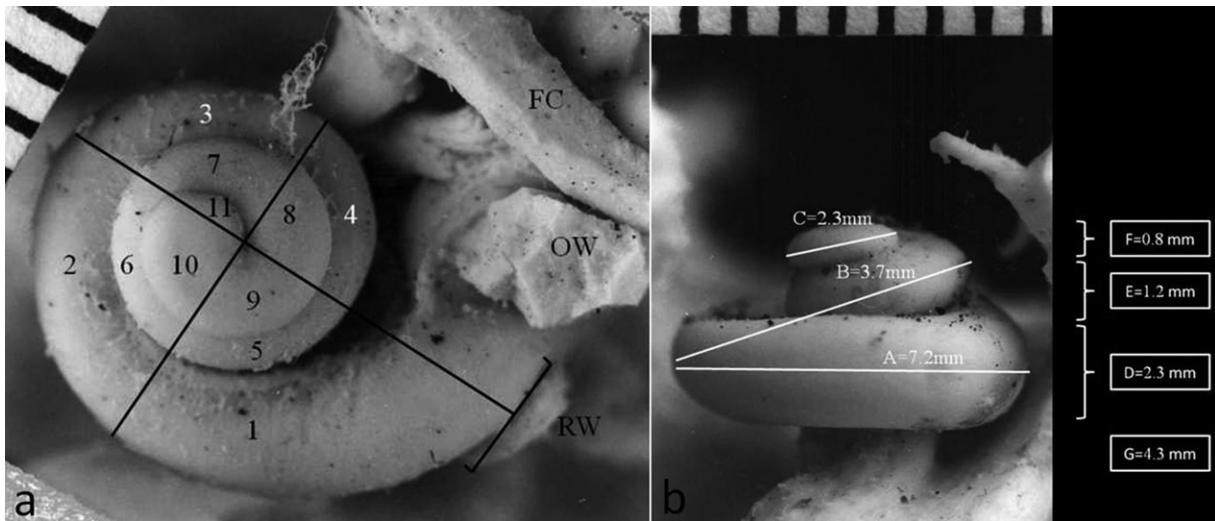
Fig. 3. (**a**) Corrosion cast from silicone material of a left side human cochlea.** Reference points used for measuring the different quadrants and turns are shown. OW, oval window; RW, round window; FC, facial canal (lifted up). (**b**) Corrosion cast of human cochlea showing angulation of the second turn. (From Erixon et al., 2009.)
[**Casting of the human cochlea: We analyzed 73 of 324 archival, non-selected, adult, corrosion casts of human inner ears. Anatomic reference points were constructed from photographic reproductions taken at different angles, and various dimensions were assessed using planimetry. Anatomic variants with particular clinical/surgical interests were pinpointed (Erixon et al., 2009). The results may assist to foresee new strategies for electric stimulation and also to better understand today's technology.]

(1538–1619) for the first pictorial delineation. In a more recent translation edited by Sellers and Anson (1962), young Scarpa's thorough description can be accessed and appreciated. They already then disagreed on the true shape of the RWM. Scarpa states that this membrane is not flat as anatomists had thought but instead conical. Scarpa proposed the term *secondary tympanic membrane* and believed that it played an even larger role for the transmission of sound into the inner ear. Adam Politzer referred to the RW membrane as the RW of Scarpa. Bast and Anson (1953) and Bollobas (1972) described its embryology in great detail.

Dimensions of the Human RW Membrane

The membrane itself has an average size of 2.3 mm × 1.87 mm according to Proctor et al. (1986) (Table 2). It does not grow postnatal. Su et al. (1982) found the minimal diameter to be 1.08 and the maximal diameter 2.28 mm based on data collected on as much as 463 specimens. Many authors do not seem to have considered the ovoid shape of the RW membrane. This can be due to the histological studies where it is difficult to realize its three-dimensional structure. The RW in human is not round but ovoid with a long and a short diameter. Adult dimensions are reached early during fetal development. Although individual values vary considerably, placement of a standard CI array with a maximum diameter of 1.0 mm through the RWM should be possible in most cases. Several electrodes today have dimensions below this size of 1 mm. RWM is formed like a saddle or "pringle-chips" (Alec Salt, oto.wustl.edu/cochlea/cachad). It consists of an infero-anterior vertical (4/7) part and a supero-posterior horizontal part (Okuno and Sando, 1988). In the posterior part, the membrane lies very close to the lamina spiralis ossea with a distance of around 0.1 mm
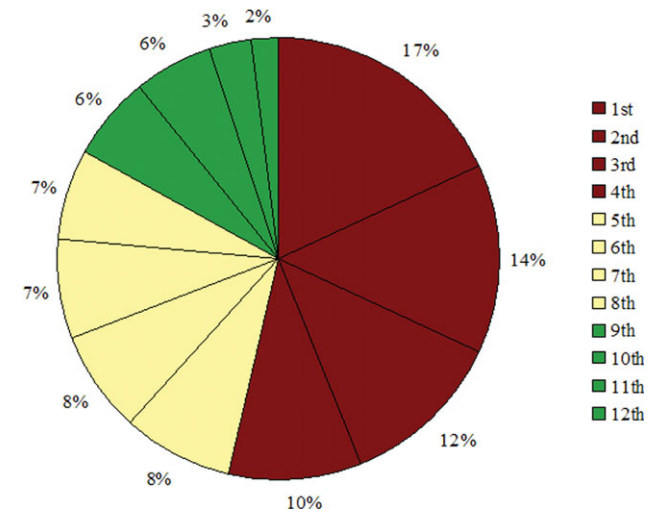

Fig. 4. Diagram showing relative lengths of various quadrants of the human cochlea. (From Erixon et al., 2009.)

(Figs. 2, 5, 6). In the center, this distance is around 1 mm (Franz et al., 1987). The thickness of the membrane varies between 50 and 100 μm and separates the fluid of the internal ear from the gas-filled space of the middle ear. The thinnest part of the RWM is the center, which can rupture if ST perilymph hydrostatic pressure rises relative to middle ear pressure. The middle ear mucosa that covers the outer surface of the RWM contains blood vessels and nerve fibers.

The RW membrane is suspended in the otic bone through a fibrous ring. The epithelium facing the middle ear is of low columnar or squamous type and
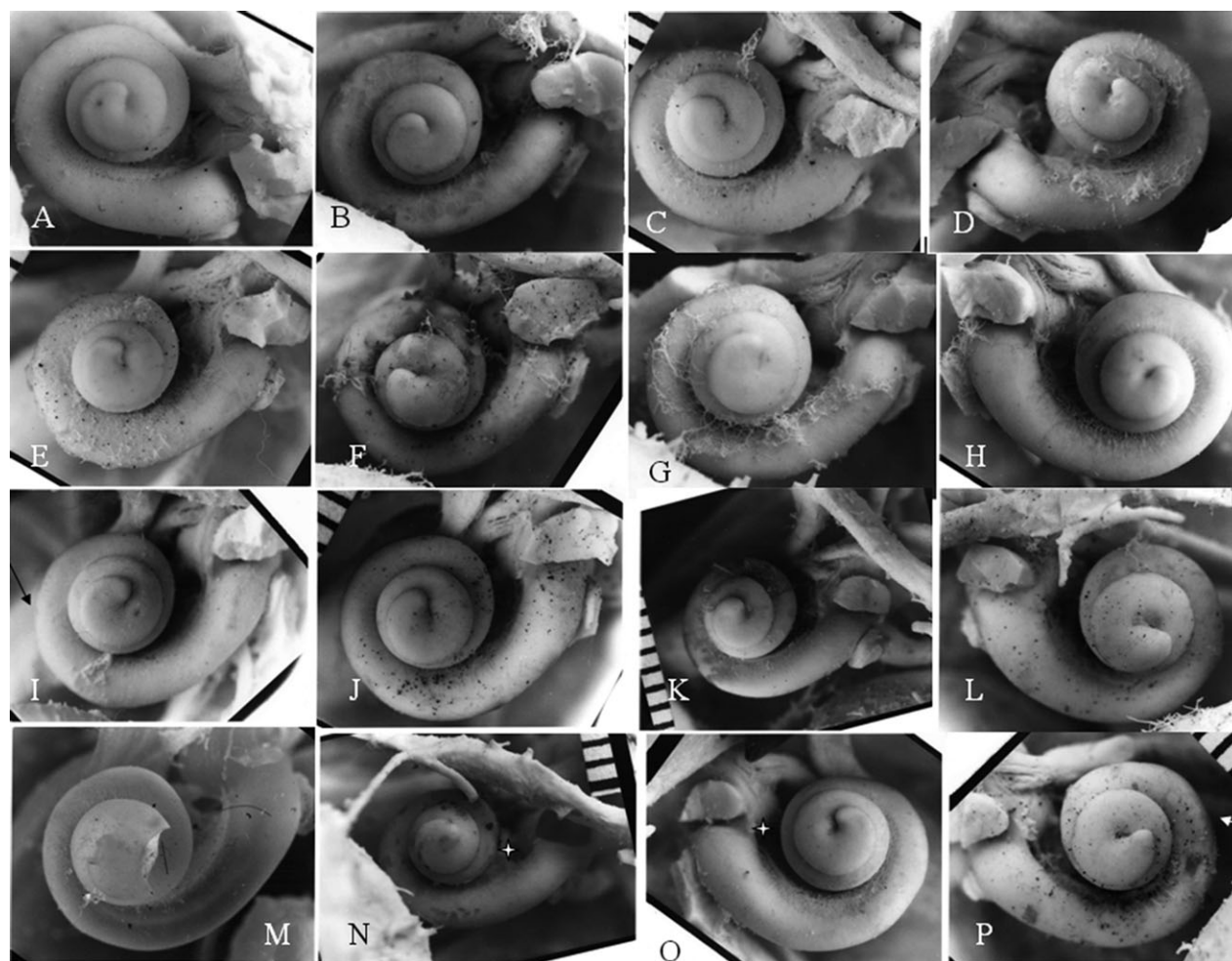
Fig. 5. Corrosion casts made from silicone and methacrylate showing different anatomy of the human cochlea. (From Erixon et al., 2009).

consists of cells held together with tight junctions and a basal lamina. There is a thin lamina propria that contains connective tissue, nerve fibers, and blood vessels (Fig. 7). A secondary membrane (pseudo-membrane) or fold usually tapers the RW niche but not always. It can be incomplete and adherent to the RWM. One must therefore be careful not to remove this membrane directly during surgery, because it can tear the RWM. A small nerve innervating the RWM from the spiral ganglion region penetrates the fibrous layer. Theoretically, and because there are morphological similarities with other mechanoreceptors in the body, it could sense and monitor perilymph pressure variations (Rask-Andersen et al., 1999; Rask-Andersen and Illing, 2004). Interestingly, these anatomical structures were not found in quadrapods, suggesting that up-right posture in humans may require additional regulatory mechanisms for fluid homeostasis (unpublished data-Rask-Andersen).

The entrance to the RWM forms a small space called the *fossula fenestrae rotunda*. Its maximal diameter is 2.98 ± 0.23 mm (Takahashi et al., 1989). Its shape varies greatly (Wysocki, 1998; Toth et al., 2006), and its

TABLE 1. The total length of the outer wall excluding the basal half of the round window (RW)

Outer wall length (mm)	Mean	Range	SD	n
Half diameter of the RW	1.1	0.3–1.6	0.21	65
First half of first turn	13.5	12.1–15.0	0.73	67
First turn (quadrant 1–4)	22.6	20.3–24.3	0.83	65
Second turn (quadrant 5–8)	12.4	10.7–13.3	0.63	63
Third turn [quadrant 9–11 (12)]	6.1	1.5–8.2	1.40	58
Total length[a]	42.0	38.6–45.6	1.96	58

SD, standard deviation; *n*, number of specimens.

appearance may puzzle the surgeon and make him believe that the RWM has been erroneously misplaced with a partly ossified entrance mistaken for the membrane itself.

Anatomy of the Facial Recess and RWM Surgery

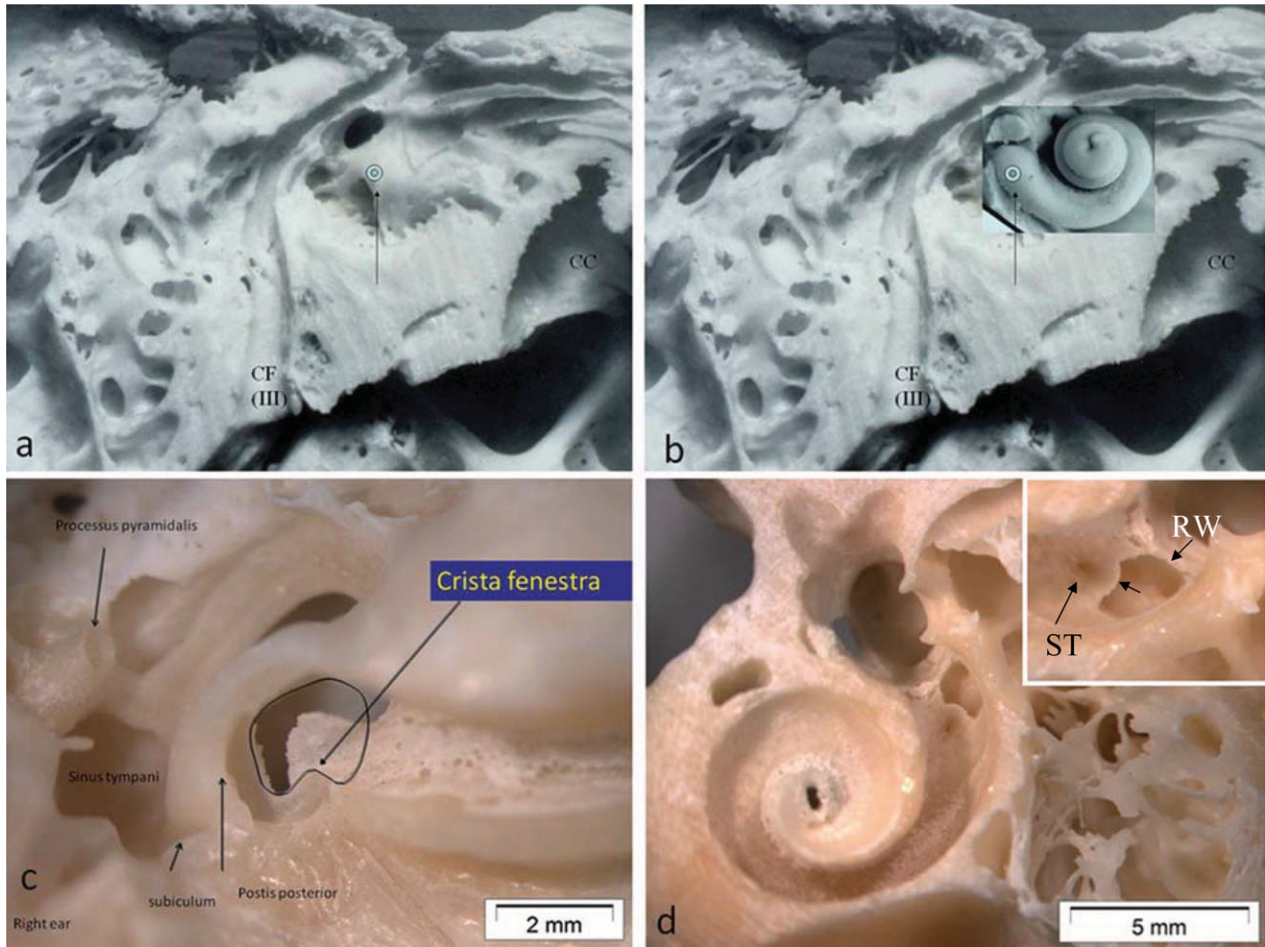The space between the lateral aspect of the third portion of the facial nerve and the chorda tympani is called

Fig. 6. (**a–d**) Microdissected human inner ears. (a, b) Microdissection of a right temporal bone showing the medial wall of the middle-ear with a positioned cochlear mold. Third portion of the facial nerve canal is shown (CF III). The position of a cochleostomy is outlined (arrows). (c) Microdissected round window region in a right human temporal bone. Subiculum and the postis posterior are shown while the postis anterior was removed to outline the RWM. The crista fenestra is seen inferiorly. (d) Dissected left side human cochlea; the round window (RW, arrow) opening can be seen from "inside" the scala tympani (ST) near the internal opening of the cochlear aqueduct (CA, arrow). Higher magnified inset illustrates the small crest that separates the aqueduct from the basal aspect of the RW, which appears "fan-like (small arrow)." Microdissected human left side inner ear.

the facial recess and is the most common pathway to the middle ear to place a CI (Fig. 8). Its size and shape can vary greatly. Sometimes, the facial nerve can protrude and make visualization of the round window membrane (RWM) impossible without removal of some part of the posterior bony wall of the meatus. The illustrations below show the various examples of the visual exposure of the RWM from the facial recess approach according to Hamamoto et al. (2000) (Fig. 9).

ELECTRON MICROSCOPY OF THE HUMAN COCHLEA—RELEVANCE FOR CI

Studies of the fine structure of the human cochlea may give us better understanding of the intracochlear tissue interacting with an electrode during insertion, at place, and during electric stimulation. Here, we used the technique of field emission scanning electron microscopy of human cochleae. SEM of hemisectioned human cochlea is

TABLE 2. Round window dimensions

Value	Species	Source
Diam 2.3×1.87	Human	Proctor et al. (1986)
Area 2.29 mm^2	Human	Okuno and Sando (1988)
Area 2.14 mm^2	Human	Su et al. (1982)

shown in Fig. 10. After decalcification, the cochlea was divided mid-modiolarly using a razor blade. It shows the typical cavities of the ST, scala vestibule (SV), and scala media (SM), or cochlear duct (Fig. 11). Variations in their shape and size are common. The pear-shaped ST at the second turn is notable, because the walls may interfere with a deep electrode insertion. Reissners membrane is very gracile and consists of both a mesothelial layer facing SV and an epithelial side facing SM (Fig. 11). The small organ of Corti rests on the BM. Some trauma was induced by the razor cut of the decalcified cochlea.
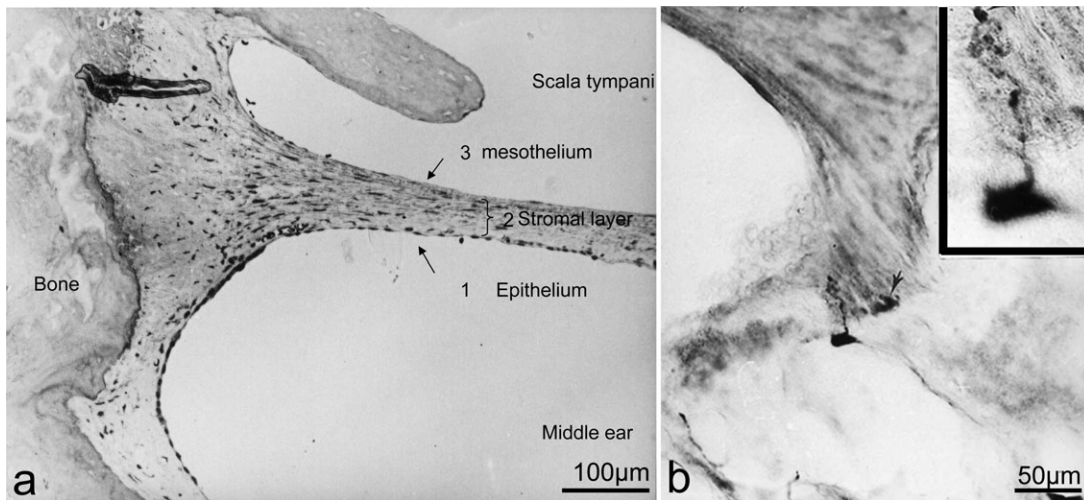
Fig. 7. Human round window (RW) membrane cryo-sectioned and stained for synaptophysin. The cochlea was harvested at surgery and fixed immediately in buffered formaldehyde. The RW membrane consists of three different layers (**a**). In (**b**) a small mechanoreceptor-like structure can be seen penetrating the RW insertion from the spiral ganglion side (magnified in inset in (b)).

Organization of the Human Cochlea

Located within the organ of Corti (Fig. 1) resides the mechanosensory cells arranged in one row of inner hair cells (IHCs) and three to four (sometimes as many as five) rows of outer hair cells (OHCs). Bundles of sensory hairs (stereocilia) emerge from the apical poles of the sensory receptor cells. Hair cells are surrounded by several types of supporting cells, and these support cells have contact with the BM. Because hair-cell stereocilia are coupled to the overlying acellular tectorial membrane, oscillations of the BM cause back-and-forth deflection of the hair bundles. This motion is not uniform along the cochlear spiral, because the BM is narrow and rather stiff on its base but is wider and more compliant near the apex of the cochlear duct. von Bekesy (1960) was the first to show that sound sets up a travelling wave and its peak amplitude varying with respect to location on the BM with frequency. High frequencies are mapped near the base while low frequencies cause maximal vibrations closer to the apex. This leads to a tonotopical organization of the sensory cells where the location of excited hair cells along the BM determines the perceived frequencies. BM and the thin Reissner's membrane (RM) subdivide the spiral canal into its three compartments. SM is filled with endolymph that can be distinguished by its ion composition that is much like an intracellular character with respect to its potassium content. ST and SV are filled with perilymph containing an extracellular-like ion composition and communicated at the apex of the cochlea via the helicotrema. The fluid contained within the tunnel of Corti and Nuel's spaces within the sensory epithelium resembles perilymph's composition.
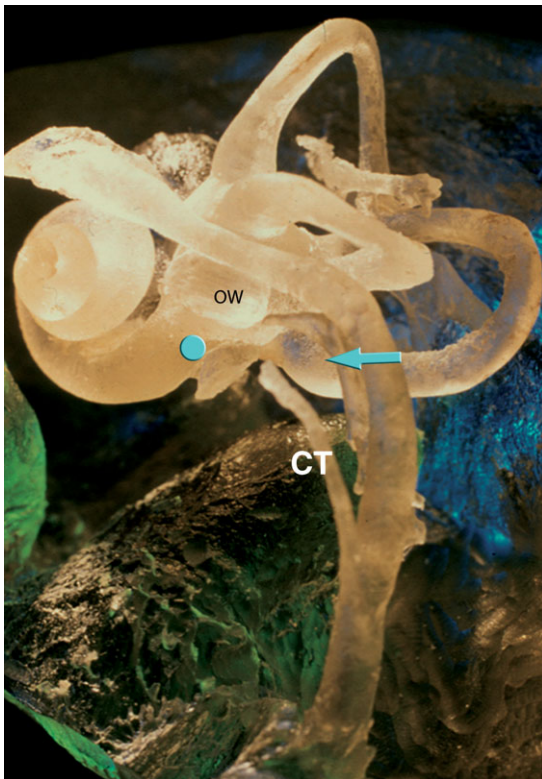

Fig. 8. Surgical anatomy of the facial recess. Plastic mold of a left human cochlea showing the topographic anatomy of the facial recess (arrow). It is located between the chorda tympani (CT) and the third portion of the facial nerve. OW, oval window. Common place for the surgeon's cochleostomy is outlined.

Reissner's Membrane

The human Reissner's membrane (RM) consists of an epithelial-cell layer facing the endolymph compartment of the SM and a mesothelial facing the perilymph compartment of the scala vestibuli (Fig. 10). These cell layers are separated by a basement membrane and form an important barrier between these two fluids that
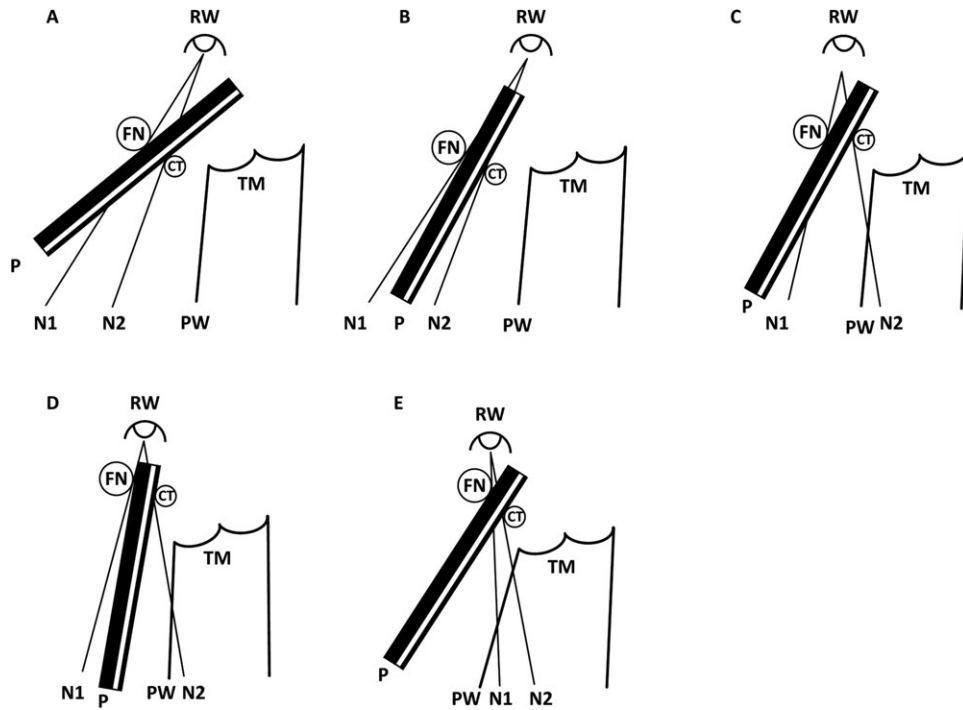
Fig. 9. The large bar shows the maximal vision angle, while the two thin lines denote the angle of exposure of the RWM. Sometimes, this angle crosses with the external ear canal like in D and E. (from Hamamoto et al., 2000).

possesses completely different ion compositions. RM is involved in homoeostasis and fluid transport. Integrity of this membrane is essential for hearing to maintain the endocochlear potential (EP; +80 mV) in the cochlear duct. In man, the membrane differs markedly from that in rodents and monkeys in that the epithelial cells have an irregular shape, and their borders make a jigsaw pattern (de Fraissinette et al., 1993) with clusters of protruding cells. Infants and children share the same uniformly polygonal surface structure of the epithelial layer (Felix et al., 1993). The function of the discontinuous mesothelial cell layer and melanocytes located almost exclusively on the perilymphatic side remain unclear. A scala vestibuli electrode insertion would most probably disrupt the patients RM and abolish the EP, thereby losing any residual hearing that may have been present.

BM and Tympanic Covering Layer

The specialized basement membrane of the sensory epithelium is a trampoline-like array of elastic fibers suspended between the modiolus and the lateral wall. It consists of mainly radial running fibrils with a characteristic rectangular shape (140 A in diameter; Kimura, 1984) embedded within a matrix. These fibers contain several different kinds of collagen (Thalmann, 1993; Cosgrove et al., 1996a,b; Dreiling et al., 2002). Furthermore, proteoglycans (Tsuprun and Santi, 2001) and fibronectins (Cosgrove and Rodgers, 1997) have been identified within the matrix.

Mechanical properties along its spiral way vary considerably and enable the tonotopical organization of the
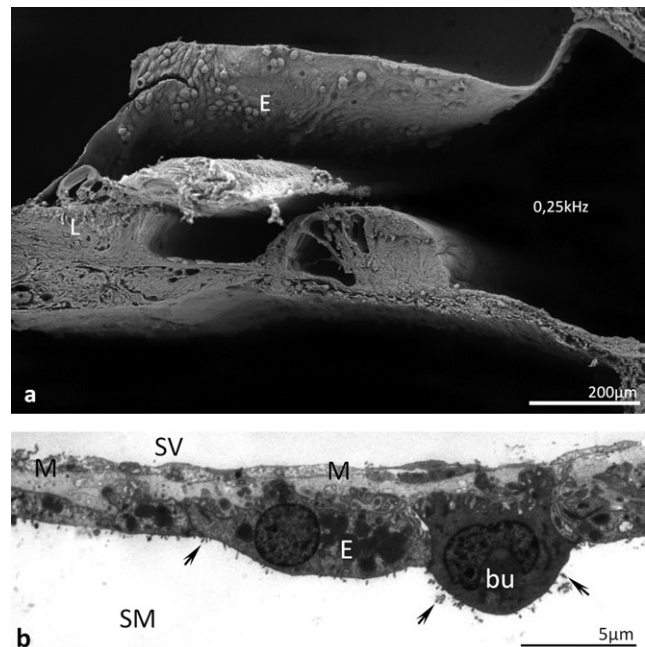
Fig. 10. (a) SEM microcraph and (b) TEM section through human Reissner's membrane displays the epithelial cell (E) layer facing the endolymph. Cells have a darker cytoplasm than mesothelial cells (M) that adheres at the perilymphatic side (scala vestibuli, SV) indicating high activity. Apical microvilli (arrows) and undulated membrane at the base suggest high transfer of molecules or ions. One epithelial cell bulges (bu) into the scala media (SM) spiral limbus (L).

Fig. 11. Lateral wall and stria vascularis in humans. (**a**) SEM*** image shows the spiral ligament. Note the thin surface la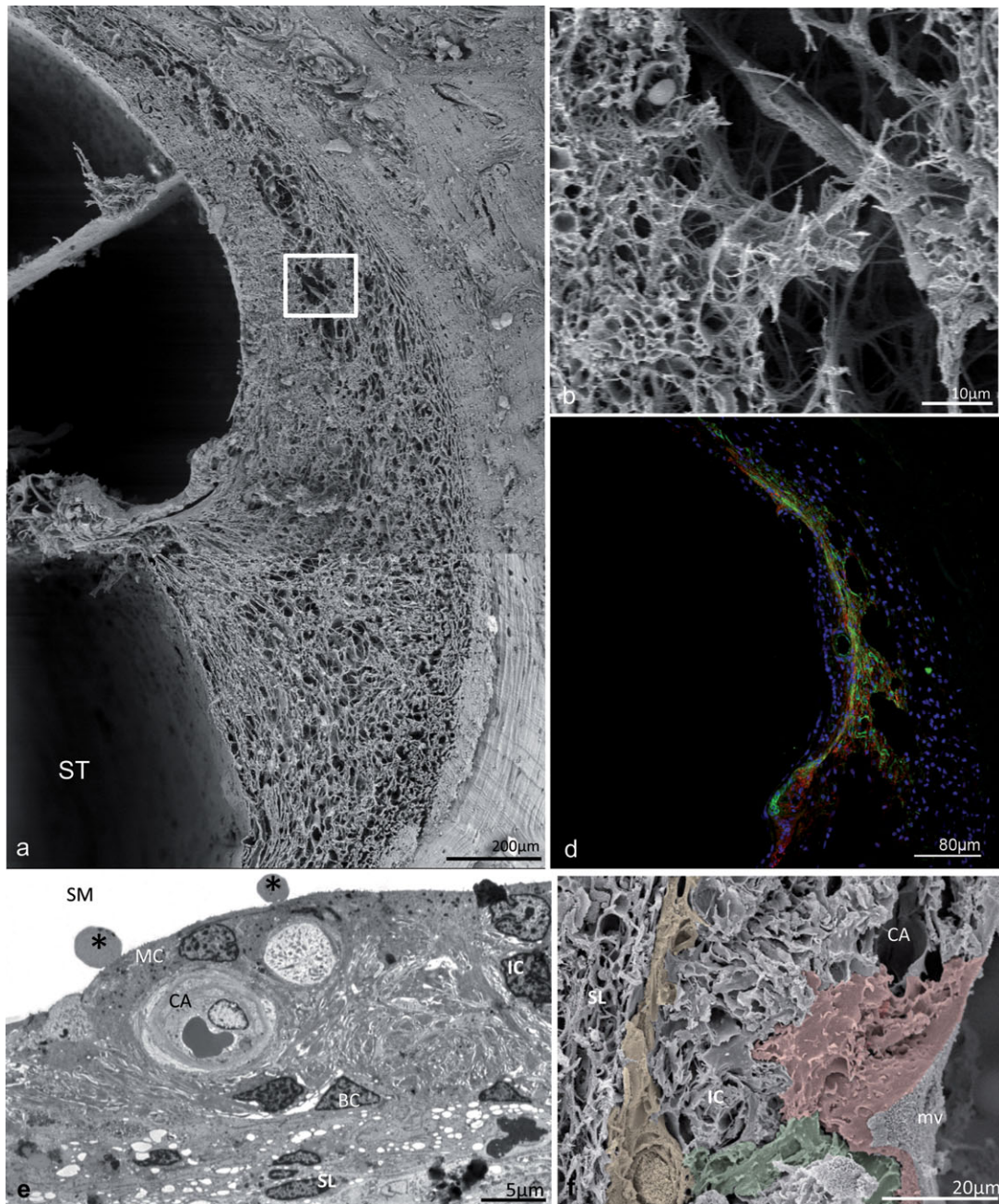yer facing scala tympani (ST) with small perforations. (**b**) Image shows a magnified view of the framed area in (**a**) demonstrating big holes in the spiral ligament frequently seen in adults. (**d**) Demonstration of connexin immunolabelling of the lateral wall of the human cochlea. Both Cx26 (red color) and Cx30 (green color) are expressed extensively at the abluminal surface of the stria vascularis. DAPI staining (blue) stains cell nuclei. These proteins play a significant role for man's hearing. Mutations in the gene that codes for Connexin 26 are responsible for up to half of all severe to profound autosomal recessive congenital deafness in many world populations (Denoyelle et al., 1997). SM, scala media. (**e, f**) SEM (e) and TEM (f) images of the human stria vascularis: three cell types arranged in consecutive layers are closely associated to the pronounced capillary (CA) system. Short microvilli (mv) line the luminal surface of the epithelial marginal cells [MC, red and green in (f)]. Intermediate cells (IC) form the medial layer and are in close contact with CAs. Flat basal cells [BC, orange in (f)] shape the boundary to the spiral ligament (SL). Membrane protrusions in the postmortem TEM tissue (asterisks) at MC are typical signs of rapid cellular degeneration.
[***The cochlea was washed in phosphate-buffered saline (PBS), pH 7.4, dehydrated in graded ethanol (70, 80, 90, 95, and 100%; 10 min each), critical point-dried, and attached to aluminium stubs. The specimens were coated in a BALTECH MED020 Coating System with gold–palladium to a nominal depth of 10–12 nm and viewed in a ZEISS DSM982 Gemini field emission electron microscope operating at 5 kV. Maximal resolution at this voltage was estimated to ~2 nm. Digital photos were taken at 1280–1024 ppi resolution. Measurements were performed using the image analysis software Image Pro 4.5.1.29 (Media Cybernetics, Inc., MD, USA).]

basilar membrane (BM). At the base, this membrane is narrow and thick (0.1 mm), and it gets thinner and broadens toward the apex (0.5 mm). Therefore, the risk of perforation of the BM with an electrode array increases with depth of insertion. The portion of the BM between the tunnel of Corti and the osseous spiral lamina forms a continuous membrane with small apertures for the passage of nerve fibers to the organ of Corti, that is, the "habenulae perforatae," while parallel strands that are peripheral to this area are free to vibrate. Along the ST, a cellular layer of tympanic covering cells that posseses phagocytic properties adheres to the thick matrix of the BM. It is possible that these cells react with the electrode by inducing a foreign body reaction leading to the formation of a fibroblast cover encasing the CI electrode. A robust proliferation of these encasing fibroblasts could lead to increased electrode impedances that can result in lower performance.

Spiral Ligament

Designation as a ligament is an awkward denomination for this highly metabolically active and important tissue. The spiral ligament anchors the BM at the lateral aspect of the otic capsule. This attachment to the organ of Corti is characterized through the presence of tension fibroblasts that contain actin, myosin, and tropomyosin. This may generate a certain active tension that can be modulated (Henson and Henson, 1988). Besides its mechanical function, the spiral ligament plays an important role for the supply and drainage of perilymph. The spongiform appearance pervaded with an extensive capillary network suggests intense high level of communication between the ST and scala vestibuli. Therefore, the spiral ligament can be assigned to the domain of the perilymphatic compartment. The importance of this tissue for maintaining the ion balance is supported through the presence of gap junctions (connexins) and Na^+/K^+-ATPase pumps. The spiral ligament is thought to pump K^+ out of the perilymph and transport it for maintaining the high concentration of K^+ in the endolymph (Spicer and Schulte, 1991; Raphael and Altschuler, 2003). High-resolution SEM of mid-modiolar section of the human cochlea displays the interior surface anatomy of the lateral wall of the ST (Fig. 11a,b). This is where the tip of the electrode first reaches the spiral ligament at the junction between the lower and upper basal turn. This is a critical step during the CI insertion with risks for perforation of this very important structure, that is, the spiral ligament.

The human stria vascularis is composed of three distinct cell types in consecutive layers: marginal cells, intermediate cells, and basal cells (Fig. 11e,f). This high-metabolic tissue is served by an extensive meshwork of capillaries and forms the lateral aspect of the SM between RM and the spiral prominence. Marginal cells are derived from epithelial cells, face the endolymph lumen, and send long intermitting processes as far as the basal cells. The surface facing the endolymph lumen is exclusively formed by marginal cells and confined through tight junctions, numerous desmosomes, and varying density and size of microvilli, which border on the endolymphatic compartment of the SM (Kimura and Schuknecht, 1970; Wright, 1980a). The mesoderm-derived intermediate cells are melanocyte-like (Hilding and Ginzberg, 1977) and originate

from the neural crest. A significant difference to other epithelia is the partial absence of a basement membrane underneath marginal cells. This may facilitate a close contact to the endothelial cells of strial capillaries and adjacent intermediate cells. The stria vascularis plays an essential role for generation and maintenance of the SM's EP. High expression of Na/K-ATPase, ionic pumps, and transporters and extensive vascularization highlights its energy consuming task. The lateral wall fibrocytes contain an amazingly large number of gap junctions. They form direct intercellular pathways for small molecules, ions, and electric currents. Mutational changes of Cx26 and also Cx30 have noted to be associated with congenital type of sensorineural deafness (Kelsell et al., 1997; Cohn and Kelley, 1999). These proteins are believed to be involved in the recirculation of potassium ions from the fluid and cellular spaces surrounding the hair cells into the supporting cells distal to the organ of Corti and shunting these ions into the fibrocytes in the spiral ligament. On freshly obtained human cochleas, we have identified several types of connexins in the organ of Corti and lateral wall tissues (Liu et al., 2009). Cx26 and Cx30 were found to be mostly coexpressed, suggesting that connexons in man consist of both types of these connexin proteins forming the channel (Fig. 11d). The exact molecular build-up in the human cochlea remains obscure. Connexin 26 was analyzed in human fetal cochlea by Kammen-Jolly et al. (2001). Connexin 43 mutations have been found to be associated with non-syndromal, autosomal, recessive deafness (Liu et al., 2001).

Tectorial Membrane

Tectorial membrane (TM) is an extracellular matrix that causes a shearing motion to stereocilia bundles when vibration enters the cochlea partition (Fig. 12). This auxiliary mass is required to present movement to the "light weight" and therefore rather vibration-insensitive hair cells. The TM is composed of radially running unbranched fibrils of type II and type IX collagen (type A) and highly branched fibers of type V collagen (type B) in which the thick fibers are embedded (Slepecky et al., 1992a,b,c). The jelly-like matrix is composed of various glycoproteins, for example, the tectorins and otogelin. Mutations in human α-tectorin underlie two dominantly inherited non-syndromic deafnesses, that is, DFNA8 and DFNA12 (Verhoeven et al., 1998). Stereocilia imprints from the OHC tallest stereocilia tips indicate a rather close attachment of these structures to the TM, while this close association between IHC stereocilia tips and the TM remains unclear. Stereocilia imprints as far as the distal end of marginal pillars suggest a different excitation for the last row of OHCs (Fig. 12b; Glueckert et al., 2005). Imprints of the IHCs and stereocilia tips on the human TM were described by Hoshino (1981). In our SEM studies, we did not observe any signs of imprints on the TM area of Hensen's stripe where the tips of the IHCs stereocilia seem to attach. There is no evidence that TM forms after birth in the human cochlea.

SUPPORTING CELLS

Supporting cells provide tight and buckling resistant connections of hair cells with the BM. The most rugged of these support cells are the inner and outer
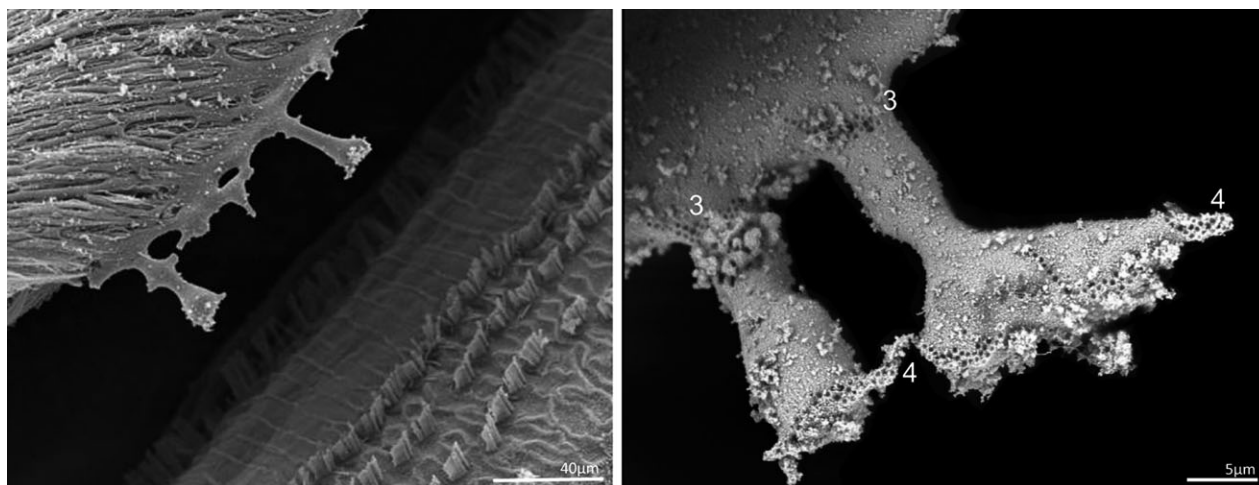
Fig. 12. SEM showing the surface of the organ of Corti with stereocilia tufts and the tectorial membrane. Note the marginal columns with impressions from the OHS stereocilia tips of the third (3) and fourth (4) row.

pillar cells that contain a massive array of specialized tubular filaments (tonofibrils) that form the tunnel of Corti. Deiter cells sustain the bases of OHCs forming a "seat" for the basal portions of these sensory cells and send a phalangeal process to the reticular lamina completing their structural support. Hensen, Claudius, and Boettcher cells shape the lateral segment of the organ of Corti. Undulated lateral-cell membranes of Hensen and Claudius cells provide surface enlargement (Glueckert et al., 2005). Supporting cells provide more than only a mechanical function. Ion transporters and a well-expressed gap-junction system serve to maintain homoeostasis and enable the support cells to act in concert. Connexins play an important role to interconnect this organized system of support cells (Fig. 13). Gene products for several ion channels such as Kcc4 (Boettger et al., 2002) have been localized to supporting cells. Potassium that enters hair cells during transduction needs to be transported back to the endolymph to maintain the high-electrochemical gradient between endo- and perilymph. K^+ channels and gap junctions are therefore needed to recycle potassium via hair cells, supporting cells, fibrocytes, and stria vascularis to the SM. Innervation of Deiters' and Hensen's cells has been described in the organ of Corti of several mammalian species (Wright and Preston, 1976; Fechner et al., 1998, 2001).

Hair Cells and Innervation

Two types of mechanotransductory sensory cells are present in the organ of Corti typically arranged in a single row of inner (IHCs) and three to four (sometimes even 5 rows of irregularly arranged OHCs in the apical region) rows of OHCs (Fig. 14). The distribution of ~3,400 IHCs and 12,000 OHCs is less regular than in lower mammals with seemingly missing OHCs and supernumerary IHCs (Wright et al., 1987; Glueckert et al., 2005). Correlative studies of hair cell density and cochlear length were performed by Ulehlova et al. in 1987. A great variability in

the length of the cochlear duct was found ranging from 28.0 to 40.1 mm. Average densities of the inner and outer hair cells decreased with increasing cochlear length with long cochleae having a greater number of hair cells in a given frequency region. These polarized neuroepithelial cells reveal specialized microvilli at their apical pole called stereocilia. These cudgel-shaped rigid (*greek: stereos*) cell protrusions contain a high amount of parallel-striated actin and are therefore unable to move like "real cilia." This rigidity of the stereocilia decreases from base to apex and may be associated with declining resonance frequencies. Several proteins have been identified in animals that play an important role in interconnecting and maintaining the actin scaffold of the stereocilia (Flock et al., 1986; Slepecky and Ulfendahl, 1992). Mutations in the gene coding for the unconventional myosin VIIa that is only expressed in stereocilia cause deafness in humans. Stereocilia are anchored into the apical pole of the hair cells with electron-dense actin rootlets in the cuticular plate. This organelle, that is, cuticular plate is a thick terminal web with high content of actin and associated proteins, with the exception of the region of the basal body, which is called cuticular pore. Stereocilia are cross-linked among each other through side links that enables them to deviate in the same direction in concert. At their apical end, thin-tip links connect stereocilia of adjacent rows that are thought to be part of the mechanotransduction receptor channel. Apart from this common organization of the receptor pole, there are significant differences between the two types of auditory hair cells (Fig. 16).

Inner hair cells.

A single inner hair cell (IHC) posseses approximately 50-70 stereocilia at the basal end and 100 in the apex of the cochlea partition (Glueckert et al., 2005; Wright, 1984) IHCs are the primary afferent sensory cells of hearing. Each IHC is innervated by several afferents that are assumed to originate exclusively from large (type I) neurons in the spiral ganglion (Fig. 16). More than 90% of
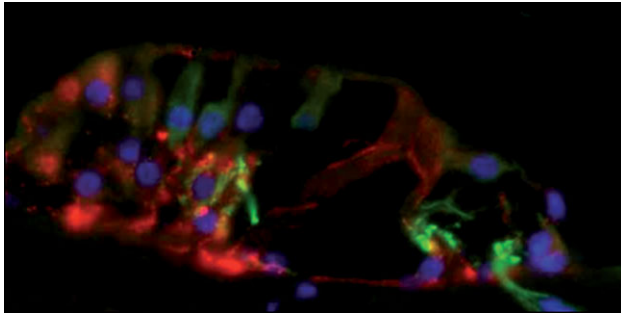
Fig. 13. Co-immunolocalization of connexin 30 (red) and neurofilament 160 (green) in the organ of Corti of man.

Fig. 14. (**a,b**) Principal nerve supply of the audtiory system (modified from Spoendlin). (a) Radial innervation of the organ of Corti with radial and spiral nerve fibers. Afferent fibers comprise inner radial fibers (IR) innervating inner hair cells (IHC) and outer spiral fibers (OS) that travel as basilar fibers (B) to the outer hair cells (OHC) where they form synapses. The efferent fibers for the IHCs (lateral efferents) are the inner spiral fibers (IS) that form contacts mainly with IR, and OHCs are innervated by medial efferents that travel as tunnel spiral (TS) and radial (R) also called tunnel crossing fibers to the OHC. (b) Horizontal innervation schema of the organ of Corti. Solid lines represent the afferent, interrupted line the efferent innervation. Afferent neurons for the IHC are strictly radial, whereas afferent nerve fibers for the OHC show considerable spiral distribution. In contrast, the efferents for the OHC show essentially a radial distribution, whereas the efferents for the IHCs run in spiral direction. SG, spiral ganglion; IGSB, intraganglionic spiral bundle.

nerve fibers in the osseous spiral lamina are to be attributed to the large spiral ganglion cells (SGCs) reflecting the importance of IHC for afferent neurotransmission to the central auditory pathway. There is a maximum of 15 nerve fibers per IHC when compared with ∼26 nerve fibers/IHC in cats (Liberman, 1980a,b). The overall afferent innervation density is maximally 1,400 fibers/millimeter and that is very low compared to 3,000 fibers/millimeter in the cat. Each terminal has several synaptic contacts with one single IHC. As has been demonstrated in animals, these terminals in man are very susceptible to anoxia. They can react with enormous swelling as observed in postmortem material. Considerable variation in size of afferent terminals was also found in man (Nadol, 1990a). Large nerve endings frequently form multiple areas of synaptic specializations, branched, and synapsed with up to three adjacent IHCs. Electron dense specializations at the presynaptic side referred to as synaptic bars, bodies, or ribbons are a common feature in human cochlea specimens. Efferent nerve terminals only form synaptic contacts with afferent dendrites, like is the case for all mammals. Very few efferent terminals reach the cell body of the IHC.

Outer hair cells.

Very few afferent nerve fibers or basilar nerve fibers run at the basis of the tunnel to the outer hair cells (OHCs). Below the OHCs, they form the outer spiral fibers. They form huge bundles of spirally oriented nerve fibers of a group of several hundred between Deiter cells. They contain 0.1-μm-thick neurocanaliculi. A few efferent nerve fibers run through these bundles and can be easily distinguished through their larger size, neurofilaments, and "en passant" synapse with outer spiral nerve fibers.

The number of outer spiral nerve fibers increases in the upper turn to about 200 and 400 in the second turn, again reduced to 300 in the apical turn. At the base of OHCs, there are large and small afferent nerve endings. Possibly, the extensive system of outer spiral fibers may interconnect or synchronize groups of OHCs enhancing the organ of Corti responses of auditory stimuli. Another difference with regard to the animal cochlea is the fewer inner spiral efferent nerve fibers and efferent nerve endings at the base of the OHCs.

Immunohistochemical investigations of the human inner ear were performed in the last decade using anti-
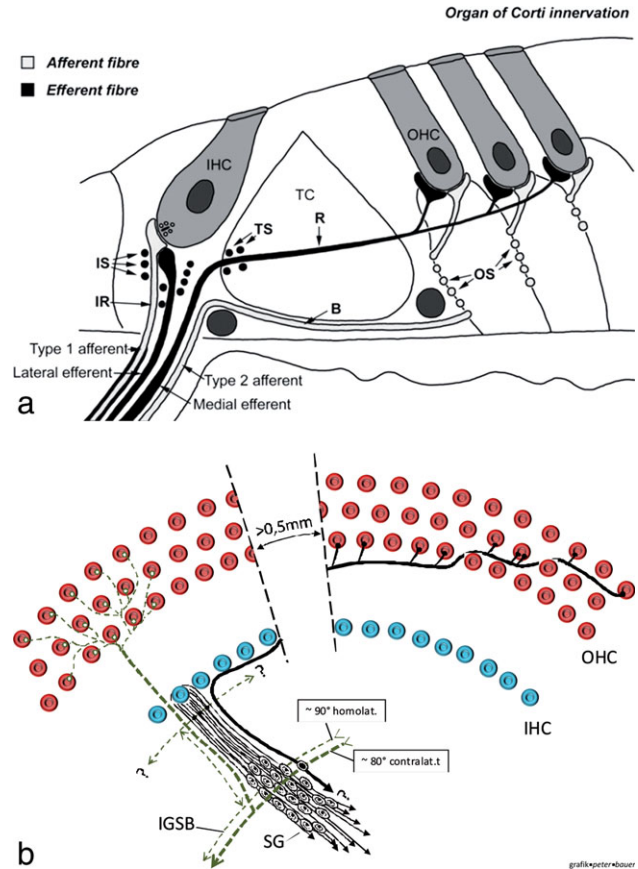
bodies against several different neurotransmitter proteins. GABA and acetylcholine have been demonstrated as efferent neurotransmitters of the human inner ear (Schrott-Fischer et al., 1994, 2002a). Glutamate-like immunostaining has also been detected in the human cochlea (Schrott-Fischer et al., 1994). The efferent cochlear nerve bundle and fiber population of the vestibulocochlear anastomosis were described in man by Gacek in 1961 and Arnesen in 1984.

Sensory Transduction and Cochlear Amplification

Hair cells are secondary sensory cells and therefore unable to generate an action potential. They
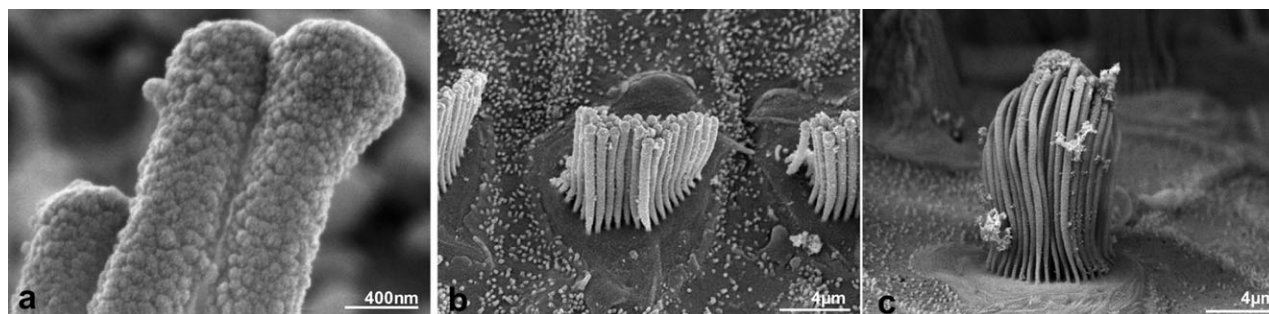
Fig. 15. (**a**) Human inner hair cell sterocilia—low-frequency region. (**b**) Outer hair cell stereocilia—high-frequency region. (**c**) Outer hair cell stereocilia–low-frequency region.

communicate their responses to the central nervous system via their afferent nerve contacts to the type I SGCs in the cochlea that are able to generate spike potentials. These SGCs are located in the modiolus, most of them within Rosenthal's canal (basal turn), and send their peripheral processes via the osseous spiral lamina to the hair cells within Corti's organ. Although less numerous, the IHCs are the main sensory cells, providing synaptic input to 90–95% of the afferent nerve fibers of the major big type I SGCs. Small type II ganglion cells are also afferent but comprise only 5–10% of all spiral ganglion neurons and are thought to innervate only the OHCs. (Spoendlin, 1979, 1985; Spoendlin and Schrott, 1989) (Fig. 14) The motor protein prestin (Zheng et al., 2000; Dallos et al., 2006, 2008) enables OHCs to rapidly change both the length and the stiffness of their cell body as their main response to sound. This motile reaction may amplify the movement of the organ of Corti, increasing sensitivity and thereby contributing to frequency analysis and binaural acoustic localization. Immunohistochemical demonstration and localization of prestin in human OHCs were recently reported (Liu et al., 2009; Fig. 17a–c).

HUMAN SPIRAL GANGLION—ANATOMY

The human cochlea from normal hearing individuals contains ∼35,000 afferent neurons that are bipolar with soma (SGCs) located in the helical Rosenthal's canal (RC) in the modiolus along the 1$\frac{3}{4}$ turns of the cochlea. The spiral ganglion terminates in a bulge containing the cell bodies of neurons innervating hair cells of the third turn (Ariyasu et al., 1989; Pamulova et al., 2006). Peripheral processes (named axons or dendrites) run within a bilamellar bony space of the osseous spiral lamina to the habenula perforata to exit this bony canal and innervate the hair cells (Fig. 18) (Rask-Andersen et al., 2006). At least two types of SGCs can be distinguished. Ninety percent can be assigned to large neurons (or type I; ∼20–30 μm in diameter). They are characterized by prominent nucleoli with loose chromatin and a cytoplasm rich in mitochondria and a well-developed endoplasmic reticulum (Rask-Andersen et al., 1997). Five to ten percent of SGCs are smaller neurons (or type II cells; ∼10–15 μm in diameter) with a nucleus that has less-pronounced heterochromatin, and the cytoplasm contains fewer mitochondria and neurofilaments. Morphological evidence of even three types of SGCs in the human was demonstrated (Nadol, 1990b; Rosbe et al., 1996). Small neuronal cells are believed to innervate the

OHCs, while the large neuronal cells innervate the IHCs (Spoendlin, 1978, Spoendlin and Schrott, 1988, 1989). Efferent nerve supply is provided from the medial and lateral olivocochlear system with fibers running spirally within RC as the so-called intraganglionic spiral bundle. It contains smaller myelinated and unmyelinated efferent nerve fibers and are closely associated with smaller (type II) neuronal cells in the peripheral portion of RC. There are also adrenergic fibers running along blood vessels and some independent of blood vessels that are intimately related to the afferent nerve fibers. The smaller spiral ganglion neurons express the protein peripherin (Liu et al., 2010).

A characteristic feature of human SGC somata is their lack of a compact myelin layer around their perikarya (Fig. 19). Some myelination can be observed more frequently in cochlea specimens from elderly people than in specimens obtained from neonates (Arnold, 1987a,b). Ota and Kimura (1980) found that both large and small neurons were myelinated and unmyelinated. However, a majority of the population was unmyelinated (94%). According to Rattay et al. (2001a,b), this would indicate a slower electric conduction rate over the SGN region in man, and, theoretically, it would take a spike more than 0.3 ms to pass the unmyelinated soma and to arrive at the central terminating process. But, as recently discussed, this could be advantageous for generation of synchronous activity important for generation of complex speech signals allowing cross-excitation (Tylstedt and Rask-Andersen, 2001). In humans, SGCs form clusters or groups (Spoendlin and Schrott, 1990; Tylstedt and Rask-Andersen, 2001a) of neuronal cells that may embody innervation of tonotopically distributed hair cells. Each IHC receives synaptic contacts from 10 to 14 neurons (Spoendlin and Schrott, 1988). These groups of neurons may act in concert in the processing of electrical signals from corresponding hair cells forming "functional units." Ganglion cells are not infrequently surrounded by common and incomplete satellite cells that could make electric cross excitation possible. Neural interactions were also found between nerve fibers and large cells as well as axosomatic connections between efferent and small ganglion cells (Rask-Andersen et al., 2000; Tylstedt and Rask-Andersen, 2001b). Nerve fiber synapses on SGCs in the human cochlea were observed by Kimura et al. (1979). Axosomatic synapses were observed on type II SGC in human (Arnold et al., 1980; Arnold, 1982a,b) and monkey (Kimura et al., 1987) but have rarely been found in lower vertebrates (Ivanov
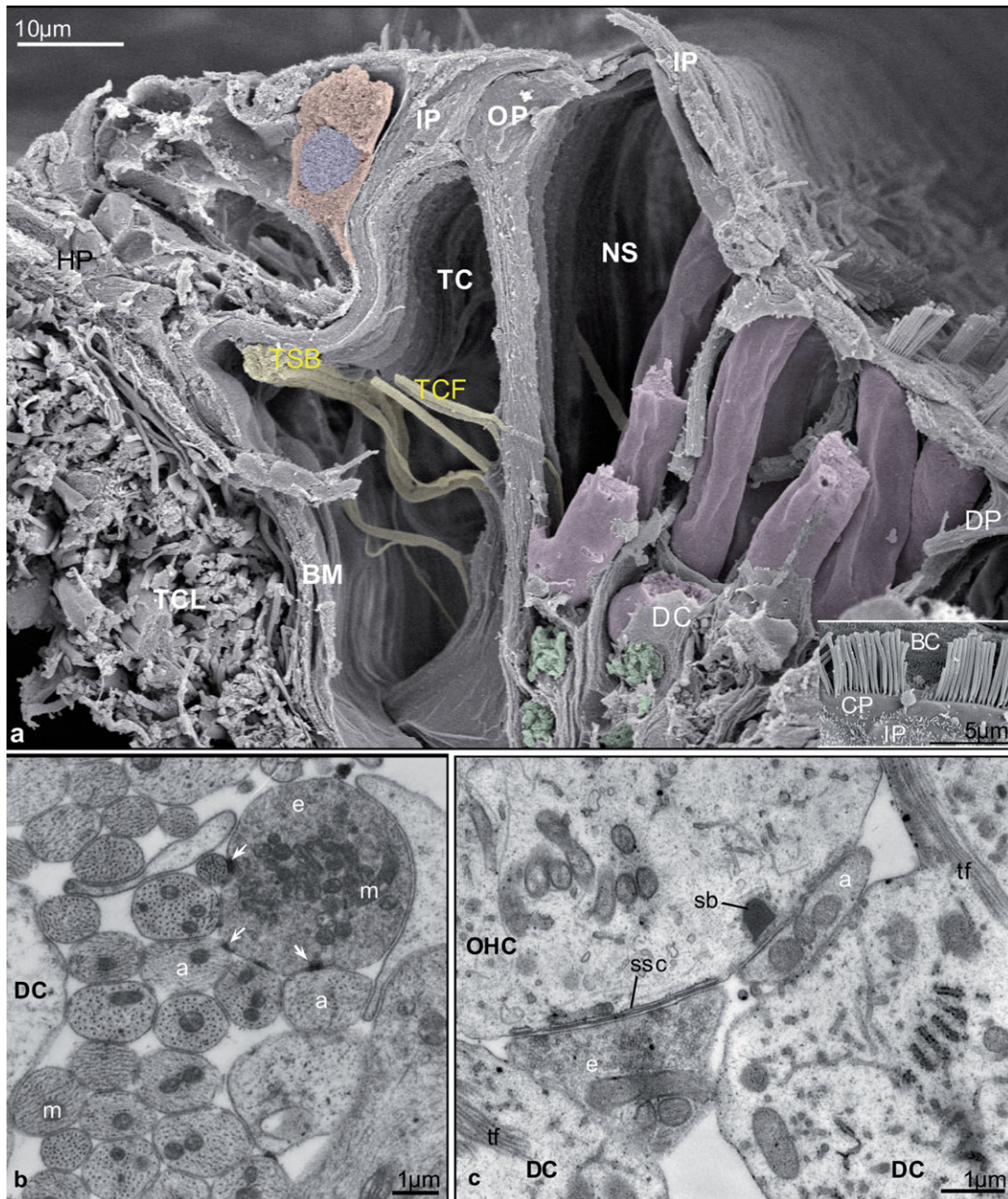
Fig. 16. (**a**) SEM view of the human organ of Corti (∼500 Hz–1 kHz region) with selected constituents colored. The inner pillar cell (IP) has partly collapsed due to a compression artefact. The tunnel of Corti (TC) between inner and outer pillar (OP) and Nuel's space (NS) are filled with a perilymph-like fluid that bathes the lateral aspect of outer hair cells-OHCs (colored pink) and Deiter phalanges (DP). OHCs rest with their base on a "seat" formed by the perikaryon of Deiter cells (DC) that hide most synaptic contacts from nerve fibers. Underneath, OHCs prominent outer spiral bundles (colored green) travel between DCs. Putative efferent fibers (colored yellow) include the tunnel spiral bundle (TSB) and radially running tunnel crossing fibers (TCF). All fibers enter the organ of Corti through small openings of the basilar membrane called habenulae perforatae (HP), thereby loosing their myelin sheet if formed. On the scala tympani side of the BM, a thick tympanic covering layer composed of several strata is attached. The inner hair cell (perikaryon colored red, nucleus colored blue) is surrounded by the IP and border cell (BC). Inset: apical pole of inner hair cells: stereocilia emanate from the cuticular plate that serves to anchor their actin rootlets. (**b**) TEM of outer spiral fibers, putative afferent fibers (a) contain many neurocanaliculi (black dots in the axoplasma seen in cross sections). Putative efferent fibers (e) are often bigger and contain neurotubules rather than neurocanaliculi that are more homogenously distributed within the axoplasma. Many mitochondria (m) probably provide energy for putative synaptic contacts between afferent and efferent fibers (arrows). (**c**) TEM of the basal pole of an outer hair cell (OHC) showing efferent (e) and afferent (a) synapses. The efferent terminal is characterized by numerous synaptic vesicles and subsurface cisterns (ssc) at its postsynaptic side. At the afferent nerve ending, synaptic vesicles are cumulated to the synaptic body (sb). tf, tonofilaments.
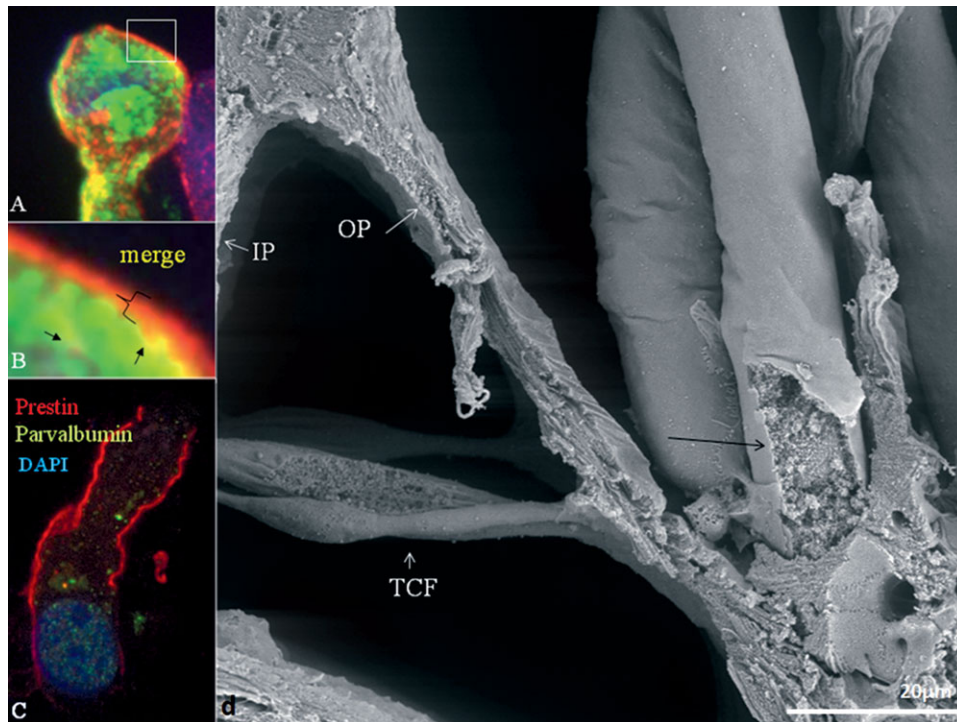
Fig. 17. Prestin immunolocalization in human outer hair cells (Reprinted with permission from Audiological Medicine 2010). IP, inner pillar cell; OP, outer pillar cell; TCF, tunnel crossing fiber (efferents). (**a**) Confocal microscopy**** of OHC expressing parvalbumin (green) and prestin (red). (**b**) Framed area in (a) in higher magnification. Prestin is expressed in the plasma membrane forming a layer of ~3–400-nm thickness. Some expression is seen in the cytosol (small arrows). (**c**) Longitudinal section. There is little expression in the inferior pole of the cell. Blue: DAPI nuclear staining.

[****The cochlea was washed in phosphate buffered saline (PBS), pH 7.4, dehydrated in graded ethanol (70, 80, 90, 95, and 100%; 10 min each), critical point dried, and attached to aluminium stubs. The specimens were coated in a BALTECH MED020 Coating System with gold–palladium to a nominal depth of 10–12 nm and viewed in a ZEISS DSM982 Gemini field emission electron microscope operating at 5 kV. Maximal resolution at this voltage was estimated to ~2 nm. Digital photos were taken at 1280–1024 ppi resolution. Measurements were performed using the image analysis software Image Pro 4.5.1.29 (Media Cybernetics, Inc., MD, USA).]

et al., 1992). Although the physiological significance of these synapses is unknown, they could mediate presynaptic neural modulation of type II auditory neurons at the level of the spiral ganglion.

HUMAN SPIRAL GANGLION AND CI

Electric stimulation from cochlear implants evokes APs in remaining acoustic nerve fibers. Where these spikes are initiated anatomically is not known. Nerve somata or initial axonal Ranviers nodes seem probable, because preserved dendrites may not seem to influence performance as evaluated histologically in patients treated with CI. Likewise, the amount of neurons necessary is still under debate (Linthicum and Galey, 1983; Linthicum et al., 1991; Nadol et al., 2001; Khan et al., 2005; Fayad and Linthicum, 2006; Nadol and Eddington, 2006), but astonishingly few neurons (~10%) seem to be required to create speech performance, reflecting the redundancy present in the acoustic system. Thus, technical advancements seem to be needed in order to take full advantage of the potential of patients' residual neural populations. This should include novel stimulation principles, additional functional channels for enhanced frequency resolution, fine structure, and music perception. A problem is the anatomic/tonotopic compression and mismatch of the spiral ganglion neurons.

Only in the basal turn are the ganglion cells distributed in such a way that frequency-specific stimulation seems possible with today's techniques (Greenwood, 1990, 1991). More apically, the ganglion cells reach only three-fourth of a turn, while the hair cell region extends to 1 and three-fourth turns over a rather short distance. These neurons, even though tonotopically arranged, cannot be selectively stimulated using current CI technique. Thus, CI stimulation or electrode insertion beyond 360° and 450° at present does not seem necessary. Also, modern technique uses monopolar stimulation that confines selective activation of neurons further questioning the need for deeper insertion of the CI electrode array. Because few data are available on the current spread in the highly anisotropic inner ear, predictions on directed stimulation of apical SGNs with a CI are difficult.

These questions are relevant to discuss in connection with new hearing-preservation techniques aiming at providing electric stimulation and hearing in the mid- and high-frequency regions. *Electroacoustic stimulation* technique uses both low-frequency acoustic hearing via the auditory hair cells and electric stimulation of preserved neurons in the same ear. Some patients may lose their residual hearing and become fully dependent on their implant for electrical stimulation of all frequencies. A deep insertion of the CI array increases the risk for loosing residual hearing but may theoretically
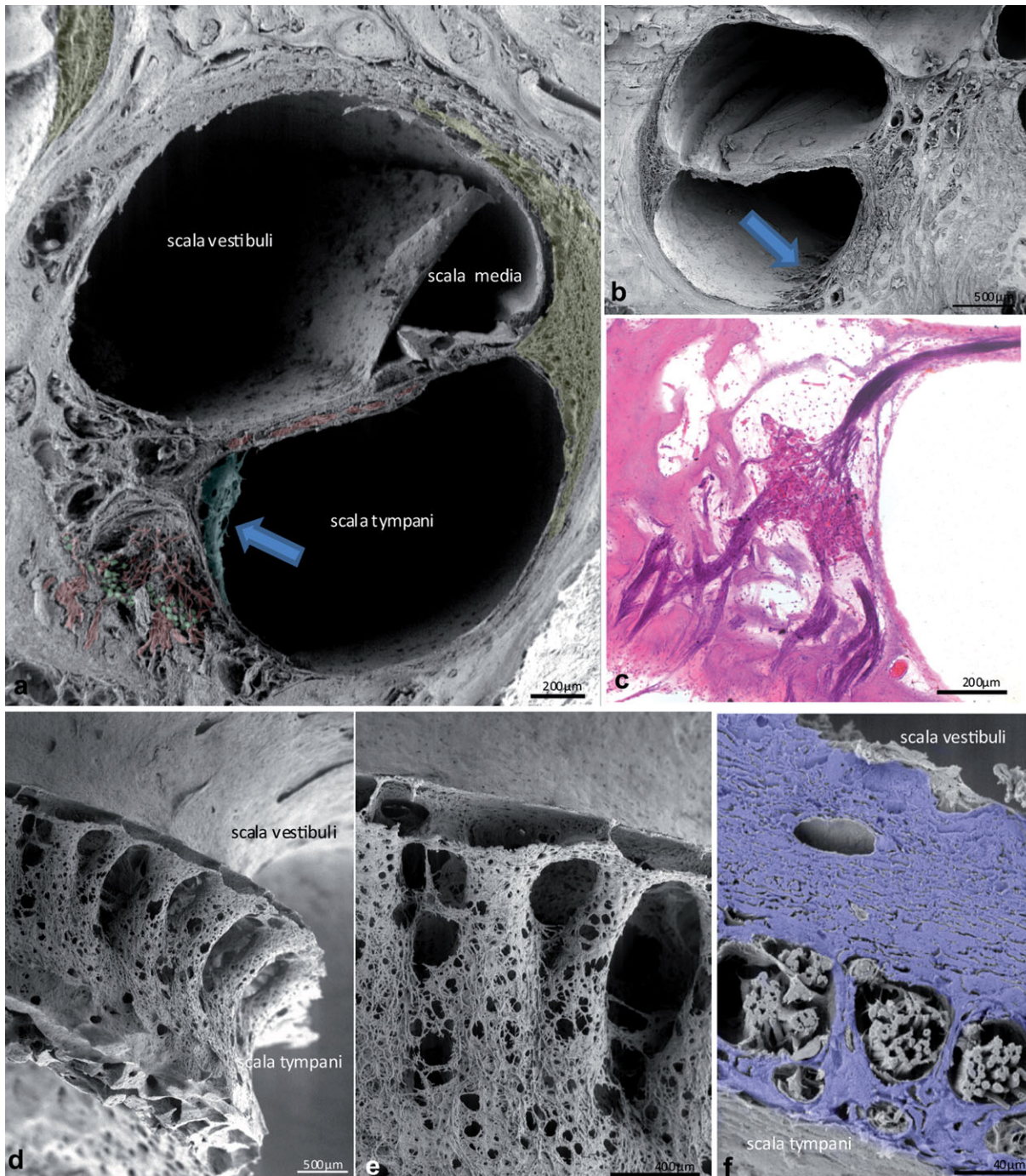
Fig. 18. (**a**) Possible trauma sites for cochlear implantation and position of neural elements in the human cochlea lower basal turn. Between scala tympani (ST) and the spiral ganglion neurons (colored green), a thin mesothelial sheet (arrow) spans between bony columns that guide nerve fibers (colored red) to the osseous spiral lamina. (**b**) At the basal aspect of ST, there are also some delicate perforated structures (arrow). Figure (**c**) displays the thin bone that separated the ST from Rosenthal's canal that houses spiral ganglion neurons. The fragile structure of the fenestrated bony columns is presented in (**d,e**). (**f**) The osseous spiral lamina bone (colored blue) comprising the peripheral axons is much thinner at the ST side.

improve performance in the case where a patient's residual hearing is eventually lost. Still, there is lacking information as to the optimal insertion depth in most cases with or without aims to preserve a patient's residual hearing.

Sensory-cell loss in animals leads to a retrograde Wallerian degeneration with a fall in the population density of the spiral ganglion's auditory neurons (Spoendlin, 1971; Schuknecht, 1993). This is believed to be caused by a disruption of neurotrophin secretion from the organ
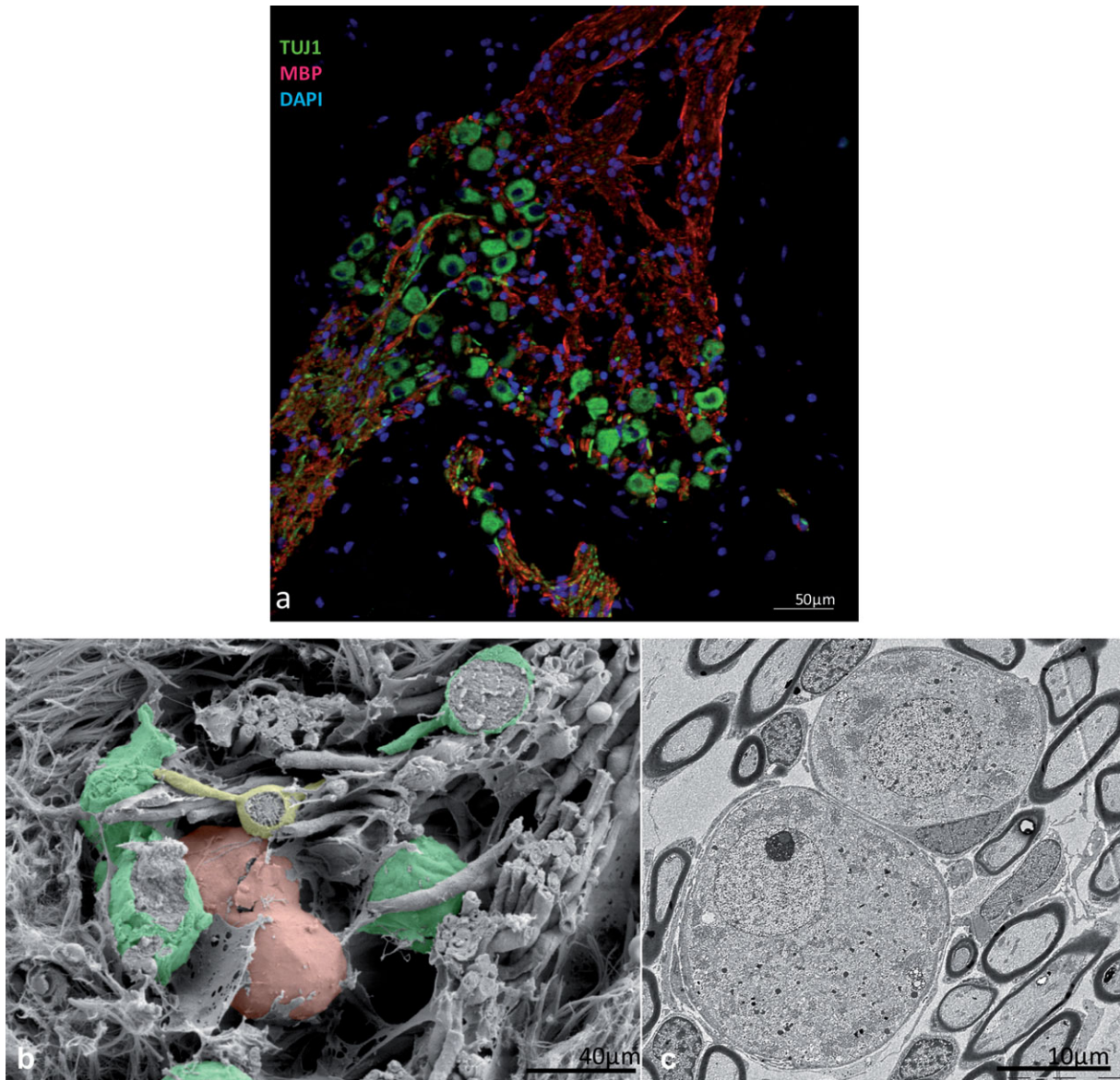
Fig. 19. Human spiral ganglion neurons: (**a**) immunohistochemistry using neural marker TUJ1 and myelin marker MBP (myelin basic protein) shows that spiral ganglia cell somata are unmyelinated. (**b**) SEM of spiral ganglion neurons in the upper basal turn. Large type 1 neuron comprise majority of nerve cells (colored green and red), only 5% are attributed to small completely unmyelinated type 2 neurons (colored yellow). Clustering of neurons (red colored) is very common in the human cochlea. (**c**) TEM of type 1 spiral ganglion neurons.

of Corti, which may act as survival factors for the associated auditory neurons. In patients with congenital deafness and adult-onset SNHL, neurons seem to be conserved even after many years of deafness. This observation suggests that there is a slower deterioration of SGCs in humans (Fayad and Linthicum, 2006). BDNF and NT-3 may be secreted by surrounding Schwann cells or satellite cells, because their receptors have been localized in the human spiral ganglion (Liu et al., 2011a,b). Also, receptors (c-ret for GDNF and isoforms) have been localized in the human spiral ganglion (Liu et al., 2011a,b; unpublished observations). It is highly plausible that several unrecognized intercellular signaling systems prevail in the human cochlea. Currently, we are focused on the surrounding satellite cell system, the unmyelination status of ganglion soma, cross-excitation, and connecting proteins, and their roles for the function, preservation, and survival of the human SGC.

Architecture of the Human Cochlea and Electrode Design—Today and the Future

An important issue is the design of various electrode arrays and how they adapt to the anatomical features of the human cochlea. Some electrode arrays are arranged close to the modiolar wall; so-called perimodiolar electrodes, while others lie free in the ST, mostly near the lateral wall (Fig. 20). Although the perimodiolar shape may result in a closer relationship between electrodes and SGC soma, it may also potentially cause trauma to
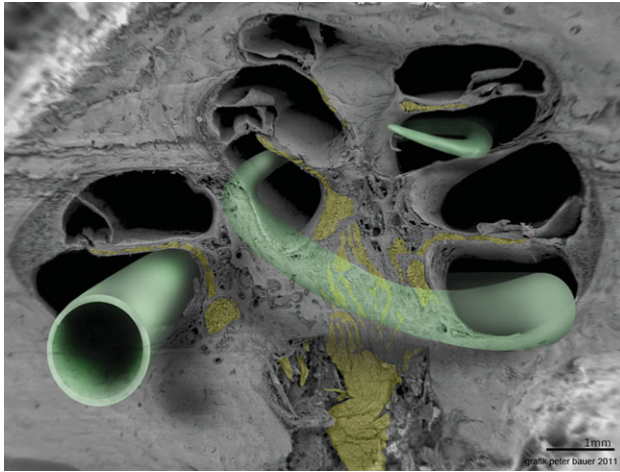
Fig. 20. SEM of a hemisectioned human cochlea. Neuronal elements are depicted in yellow. Possible electrode positions are illustrated by an electrode array in green. Different electrode designs aim a site close to the modiolus (perimodiolar-lower basal turn at the left of the figure), while non–preshaped electrodes locate closer to the spiral ligament and osseous spiral lamina (other electrode positions).

the thin bony wall of the modiolus (Rask-Andersen et al., 2006) (Fig. 18). On the other hand, a laterally positioned electrode array may cause strain to the lateral wall and BM. In revision surgery, more force may be required to extract a CI that is hugged around the modiolus. This could be a disadvantage in children who can be expected to undergo revision surgery several times during their life time. In the future, electrode designers need to shape electrodes in such a way that they minimize trauma during insertion. This is important, because trauma against the medial wall of the ST can damage the spiral ganglion, which is the prime target of electric stimulation by the electrodes of the implant. Smaller and more flexible arrays will be needed to adjust to the individual structural variations in the design of the human cochlea and for preserving the residual hearing of individual patients.

LITERATURE CITED

Agterberg MJ, Versnel H, de Groot JC, van den Broek M, Klis SF. 2010. Chronic electrical stimulation does not prevent spiral ganglion cell degeneration in deafened guinea pigs. Hear Res 269:169–179.

Albini BS. 1744. Explicatio tabularum anatomicarum, *Leidae Batavorum* [Leyden]. Albinus, BS, Eustachi, B. Apud Joannem Arnoldum Langerak, et Joannem & Hermannum Verbeek, bibliop., 277pp.

Araki S, Kawano A, Seldon L, Shepherd RK, Funasaka S, Clark GM. 1998. Effects of chronic electrical stimulation on spiral ganglion neuron survival and size in deafened kittens. Laryngoscope 108:687–695.

Ariyasu L, Galey F, Hilsinger R, Byl FM. 1989. Computer-generated three-dimensional reconstruction of the cochlea. Otolaryngol Head Neck Surg 100:87–91.

Arnesen AR. 1984. Fibre population of the vestibulocochlear anastomosis in humans. Acta Otolaryngol 98:501–518.

Arnold W. 1982a. Pathogenetic reflections concerning Menière's disease. Adv Otorhinolaryngol 28:118–120.

Arnold W. 1987a. Myelination of the human spiral ganglion. Acta Otolaryngol Suppl 436:76–84.

Arnold W. 1987b. Possibilities of immunohistochemical investigation on human temporal bone. Acta Otolaryngol Suppl 436:62–68.

Arnold WJ. 1982b. The spiral ganglion of the newborn baby. Am J Otol 3:266–269.

Arnold W, Wang JB, Linnenkohl S. 1980. [Anatomical observations in the spiral ganglion of human newborns (author's transl)]. Arch Otorhinolaryngol 228:69–84. (German).

Bast TH. 1942. Development of the otic capsule. Ann Otol Rhinol Laryngol 51:343–357.

Bast TH, Anson BJ. 1953. The temporal and bone and the ear. Springfield, IL: Thomas.

Bagger-Sjöbäck D, Engström B. 1985. Preservation of the human cochlea. Ann Otol Rhinol Laryngol 94:284–292.

Biedron S, Prescher A, Ilgner J, Westhofen M. 2010. The internal dimensions of the cochlear scalae with special reference to cochlear electrode insertion trauma. Otol Neurotol 31:731–737.

Boettger T, Hubner CA, Maier H, Rust MB, Beck FX, Jentsch TJ. 2002. Deafness and renal tubular acidosis in mice lacking the K–Cl co-transporter Kcc4. Nature 416:874–878.

Bredberg G. 1968. Cellular pattern and nerve supply of the human organ of Corti. Acta Otolaryngol 236:1.

Bredberg G, Lindeman HH, Ades HW, West R, Engstrom H. 1970. Scanning electron microscopy of the organ of Corti. Science 170:861–863.

Bollobas B. 1972. A halloszerv microchirurgiai anutomiaja. Budapest: Medicina Könyvkiado.

Burian K, Hochmair-Desoyer IJ, Hochmair ES. 1981. Hoeren uber ein cochleaimplantat. Arch ONK-Heilk 231:569–570.

Corti A. 1851. Recherches sur l'organe de l'ouie des mamiferes. Z Wiss Zool 3:109–106.

Clark GM. 1975. A surgical approach for cochlear implants. J Laryngol Otol 89:9–15.

Clark GM, Pyman BC, Bailey OR. 1979. The surgery for multiple electrode cochlear implantation. J Laryngol Otol 93:215–223.

Coco A, Epp SB, Fallon JB, Xu J, Millard RE, Shepherd RK. 2006. Does cochlear implantation and electrical stimulation affect residual hair cells and spiral ganglion neurons? Hear Res 225:60–70.

Cohn ES, Kelley PM. 1999. Clinical phenotype and mutations in connexin 26 (DFNB1/GJB2), the most common cause of childhood hearing loss. Am J Med Genet 89:130–136.

Cosgrove D, Rodgers KD. 1997. Expression of the major basement membrane-associated proteins during postnatal development in the murine cochlea. Hear Res 105:159–170.

Cosgrove D, Kornak JM, Samuelson G. 1996a. Expression of basement membrane type IV collagen chains during postnatal development in the murine cochlea. Hear Res 100:21–32.

Cosgrove D, Samuelson G, Pinnt J. 1996b. Immunohistochemical localization of basement membrane collagens and associated proteins in the murine cochlea. Hear Res 97:54–65.

Comis SD, Osborne MP, O-Connell J, Johnson AP. 1990. The importance of early fixation in preservation of human cochlear and vestibular sensory hair bundles. Acta Otolaryngol 109:361–368.

Cotugno D. 1761. *De aquaeductibus auris humanae internae anatomica dissertatio.* Neapoli, Simoniana.

Dallos P, Wu X, Cheatham M, Gao J, Zheng J, Anderson CT, Anderson CT, Jia S, Wang X, Cheng WH, Sengupta S, He DZ, Zuo J. 2008. Prestin-based outer hair cell motility is necessary for mammalian cochlear amplification. Neuron 58:333–339.

Dallos P, Zheng J, Cheatham MA. 2006. Prestin and the cochlear amplifier. J Physiol 576(Pt 1):37–42. (Review).

de Fraissinette A, Felix H, Nievergelt J, Gleeson M. 1993. Ultrastructural features of human Reissner's membrane. Scann Microsc 7:217–221.

Denoyelle F, Weil D, Maw MA, Wilcox SA, Lench NJ, Allen-Powell DR, Osborn AH, Dahl HH, Middleton A, Houseman MJ, Dodé C, Marlin S, Boulila-ElGaïed A, Grati M, Ayadi H, BenArab S, Bitoun P, Lina-Granade G, Godet J, Mustapha M, Loiselet J, El-Zir E, Aubois A, Joannard A, Petit C. 1997. Prelingual deafness: high prevalence of a 30delG mutation in the connexin 26 gene. Hum Mol Genet 6:2173–2177.

Dimopoulos P, Muren C. 1990. Anatomic variations of the cochlea and relations to other temporal bone structures. Acta Radiol 31: 439–444.

Dreiling FJ, Henson MM, Henson OW, Jr. 2002. Immunolabeling type II collagen in the basilar membrane, a pre-embedding approach. Hear Res 166:181–191.

Engstrom B, Hillerdal M, Hillerdal G. 1990. Preservation of the human cochlea with two different fixatives. Acta Otolaryngol Suppl 470:31–33.

Engstrom B, Hillerdal M, Laurell G, Bagger-Sjoback D. 1987. Selected pathological findings in the human cochlea. Acta Otolaryngol Suppl 436:110–116.

Erixon E, Högstorp H, Wadin K, Rask-Andersen H. 2009. Variational anatomy of the human cochlea: implications for cochlear implantation. Otol Neurotol 30:14–22.

Eustachius B. 1564. *Opuscula Anatomica*. Vincentius Luchinus excudebat. Venice.

Fayad JN, Linthicum FH, Jr. 2006. Multichannel cochlear implants: relation of histopathology to performance. Laryngoscope 116: 1310–1320.

Fechner FP, Burgess BJ, Adams JC, Liberman MC, Nadol JB, Jr. 1998. Dense innervation of Deiters' and Hensen's cells persists after chronic deefferentation of guinea pig cochleas. J Comp Neurol 400:299–309.

Fechner FP, Nadol JB JR, Burgess BJ, Brown MC. 2001. Innervation of supporting cells in the apical turns of the guinea pig cochlea is from type II afferent fibers. J Comp Neurol 429:289–298.

Felix H, de Fraissinette A, Johnsson LG, Gleeson MJ. 1993. Morphological features of human Reissner's membrane. Acta Otolaryngol 113:321–325.

Flock A, Flock B, Ulfendahl M. 1986. Mechanisms of movement in outer hair cells and a possible structural basis. Arch Otorhinolaryngol 243:83–90.

Franz BKH, Clark GM, Bloom DM. 1987. Surgical anatomy of the round window with special reference to cochlear implantation. J Otolaryngol Otol 108:97–102.

Fujimoto S, Yamamoto K, Hayabuchi I, Yoshizuka M. 1981. Scanning and transmission electron microscope studies on the organ of Corti and stria vascularis in human fetal cochlear ducts. Arch Histol Jpn 44:223–235.

Gacek RR. 1961. The efferent cochlear bundle in man. Arch Otolaryngol 74:690–694.

Gleeson MJ. 1985. A scanning electron microscopy study of post mortem autolytic changes in the human and rat cochleas. Acta Otolaryngol 100:419–428.

Glueckert R, Pfaller K, Kinnefors A, Schrott-Fischer A, Rask-Andersen H. 2005. High resolution scanning electron microscopy of the human organ or Corti: a study using freshly fixed surgical specimens. Hear Res 199:40–56.

Greenwood DD. 1990. A cochlear frequency-position function for several species: 29 years later. J Acoust Soc Am 87:2592–2605.

Greenwood DD. 1991. Critical bandwidth and consonance in relation to cochlear frequency-position coordinates. Hear Res 54: 164–208.

Hamamoto M, Murakami G, Kataura A. 2000. Topographical relationships of the facial nerve, *Chorda tympani* nerve, and round windowwith special reference to the approach route for cochlear implantation. Clin Anat 13:251–256.

Hardy M. 1938. The length of the organ of Corti in man. Am J Anat 63:291–311.

Hartshorn DO, Miller JM, Altschuler RA. 1991. Protective effect of electrical stimulation in the deafened guinea pig cochlea. Otolaryngol Head Neck Surg 104:311–319.

Henson MM, Henson OW, Jr. 1988. Tension fibroblasts and the connective tissue matrix of the spiral ligament. Hear Res 35: 237–258.

Hilding DA, Ginzberg RD. 1977. Pigmentation of the stria vascularis. The contribution of neural crest melanocytes. Acta Otolaryngol 84:24–37.

House WF, Urban J. 1973. Long term results of electrode implantation and electronic stimulation of the cochlea in man. Ann Otol Rhinol Laryngol 82:504–517.

Hoshino T. 1977. Contact between the tectorial membrane and the cochlear sensory hairs in the human and the monkey. Arch Otorhinolaryngol 217:53–60.

Hoshino T. 1981. Imprints of the inner sensory cell hairs on the human tectorial membrane. Arch Otorhinolaryngol 232:65–71.

Hoshino T. 1990. Scanning electron microscopy of nerve fibers in human fetal cochlea. J Electron Microsc Tech 15:104–114.

Hoshino T, Nakamura K. 1985. Nerve fibers in the fetal organ of Corti. Scanning electron microscopic study. Ann Otol Rhinol 94: 304–308.

Hunter-Duvar IM. 1975. Hearing and hair cells. Can J Otolaryngol 4:152–160.

Igarashi Y. 1980. Cochlea of the human fetus: a scanning electron microscope study. Arch Histol Jpn 43:195–209.

Ivanov E, Koitchev K, Cazals Y, Aran JM. 1992. Axo-somatic contacts in the postnatal developing white rat spiral ganglion. Acta Otolaryngol 112:985–990.

Kammen-Jolly K, Ichiki H, Scholtz AW, Gsenger M, Kreczy A, Schrott-Fischer A. 2001. Connexin 26 in human fetal development of the inner ear. Hear Res 160:15–21.

Kanzaki S, Stover T, Kawamoto K, Prieskorn DM, Altschuler RA, Miller JM, Raphael Y. 2002. Glial cell line-derived neurotrophic factor and chronic electrical stimulation prevent VIII cranial nerve degeneration following denervation. J Comp Neurol 454: 350–360.

Kawano A, Seldon HL, Clark GM. 1996. Computer-aided three-dimensional reconstruction in human cochlear maps: measurement of the lengths of organ of Corti, outer wall, inner wall, and Rosenthal's canal. Ann Otol Rhinol Laryngol 105:701–709.

Kelsell DP, Dunlop J, Stevens HP, Lench NJ, Liang JN, Parry G, Mueller RF, Leigh IM. 1997. Connexin 26 mutations in hereditary non-syndromic sensorineural deafness. Nature 387:80–83.

Kennedy DW. 1987. Multichannel intracochlear electrodes: mechanisms of insertion trauma. Laryngoscope 97:42–49.

Khan AM, Handzel O, Burgess BJ, Damian D, Eddington DK, Nadol JB Jr. 2005. Is word recognition correlated with the number of surviving spiral ganglion cells and electrode insertion depth in human subjects with cochlear implants? Laryngoscope 115: 672–677.

Khan AM, Handzel O, Damian D, Eddington DK, Nadol JB. 2005. Effect of cochlear implantation on residual spiral ganglion cell count as determined by comparison with the contralateral nonimplanted inner ear in humans. Ann Otol Rhinol Laryngol 114: 381–385.

Kimura RS. 1984. Fistulae in the membranous labyrinth. Ann Otol Rhinol Laryngol Suppl 112:36–43.

Kimura RS, Schuknecht HF. 1970. The ultrastructure of the human stria vascularis. I. Acta Otolaryngol 69:415–427.

Kimura RS, Bongiorno CL, Iverson NA. 1987. Synapses and ephapses in the spiral ganglion. Acta Otolaryngol Suppl 438:1–18.

Kimura RS, Ota CS, Takahashi T. 1979. Nerve fiber synapses on spiral ganglion cells in the human cochlea. Ann Otol Rhinol Laryngol 88:1–17.

Lavigne-Rebillard M, Pujol R. 1986. Development of the auditory hair cell surface in human fetuses. A scanning electron microscopy study. Anat Embryol (Berl) 174:369–377.

Lavigne-Rebillard M, Pujol R. 1987. Surface aspects of the developing human organ of Corti. Acta Otolaryngol Suppl 436:43–50.

Lavigne-Rebillard M, Cousillas H, Pujol R. 1985a. The very distal part of the basilar papilla in the chicken: a morphological approach. J Comp Neurol 238:340–347.

Lavigne-Rebillard M, Dechesne C, Pujol R, Sans A, Escudero P. 1985b. [Development of the internal ear during the 1st trimester of pregnancy. Differentiation of the sensory cells and formation of the 1st synapses]. Ann Otolaryngol Chir Cervicofac 102:493–498. (French).

Leake PA, Hradek GT, Rebscher SJ, Snyder RL. 1991. Chronic intracochlear electrical stimulation induces selective survival of spiral ganglion neurons in neonatally deafened cats. Hear Res 54: 251–271.

Leake PA, Hradek GT, Snyder RL. 1999. Chronic electrical stimulation by a cochlear implant promotes survival of spiral ganglion neurons after neonatal deafness. J Comp Neurol 412:543–562.

Leake PA, Snyder RL, Hradek GT, Rebscher SJ. 1995. Consequences of chronic extracochlear electrical stimulation in neonatally deafened cats. Hear Res 82:65–80.

Liberman MC. 1980a. Efferent synapses in the inner hair cell area of the cat cochlea: an electron microscopic study of serial sections. Hear Res 3:189–204.

Liberman MC. 1980b. Morphological differences among radial afferent fibers in the cat cochlea: an electron-microscopic study of serial sections. Hear Res 3:45–63.

Li L, Parkins CW, Webster DB. 1999. Does electrical stimulation of deaf cochleae prevent spiral ganglion degeneration? Hear Res 133:27–39.

Lim DJ. 1972. Fine morphology of the tectorial membrane. Its relationship to the organ of Corti. Arch Otolaryngol 96:199–215.

Lim DJ, Lane WC. 1969. Cochlear sensory epithelium. A scanning electron microscopic observation. Ann Otol Rhinol Laryngol 78: 827–841.

Linthicum FH, Jr., Galey FR. 1983. Histologic evaluation of temporal bones with cochlear implants. Ann Otol Rhinol Laryngol 92(6, Pt 1):610–613.

Linthicum FH, Jr., Fayad J, Otto SR, Galey FR, House WF. 1991. Cochlear implant histopathology. Am J Otol 12:245–311.

Liu W, Boström M, Kinnefors A, Linthicum F, Rask-Andersen H. 2011a. Expression of myelin basic protein in the human auditory nerve—an immunohistochemical and comparative study. Auris Nasus Larynx 39:18–24.

Liu W, Boström M, Kinnefors A, Rask-Andersen H. 2009. Unique expression of connexins in the human cochlea. Hear Res 250: 55–62.

Liu W, Boström M, Rask-Andersen H. 2009. Immunolocalization of prestin in the human cochlea. Audiol Med 8:56–62.

Liu W, Kinnefors A, Boström M, Rask-Andersen H. 2010. Expression of peripherin in human cochlea. Cell Tissue Res 342: 345–351.

Liu W, Kinnefors A, Boström M, Rask-Andersen H. 2011b. Expression of TrkB and BDNF in human cochlea—an immunohistochemical study. Cell Tissue Res 345:213–221.

Liu XZ, Xia XJ, Adams J, Chen ZY, Welch KO, Tekin M, Ouyang XM, Kristiansen A, Pandya A, Balkany T, Arnos KS, Nance WE. 2001. Mutations in GJA1 (connexin 43) are associated with nonsyndromic autosomal recessive deafness. Hum Mol Genet 10: 2945–2951.

Lloyd SK, Kasbekar L, Kenway B, Prevost T, Hockman M, Beale T, Graham J. 2010. Developmental changes in cochlear orientation-implications for cochlear implantation. Otol Neurotol 31:902–907.

Lousteau RJ. 1987. Increased spiral ganglion cell survival in electrically stimulated, deafened guinea pig cochleae. Laryngoscope 97: 836–842.

Martinez-Monedero R, Niparko JK, Aygun N. 2011. Cochlear coiling pattern and orientation differences in cochlear implant candidates. Otol Neurotol 32:1086–1093.

Michelson RP. 1971. Electrical stimulation of the human cochlea. Arch Otolaryngol 93:319–323.

Miller CA, Woodruff KE, Pfingst BE. 1995. Functional responses from guinea pigs with cochlear implants. I. Electrophysiological and psychophysical measures. Hear Res 92:85–99.

Mitchell A, Miller JM, Finger PA, Heller JW, Raphael Y, Altschuler RA. 1997. Effects of chronic high-rate electrical stimulation on the cochlea and eighth nerve in the deafened guinea pig. Hear Res 105:30–43.

Nadol JB, Jr. 1983. Serial section reconstruction of the neural poles of hair cells in the human organ of Corti. I. Inner hair cells. Laryngoscope 93:599–614.

Nadol JB, Jr. 1990a. Degeneration of cochlear neurons as seen in the spiral ganglion of man. Hear Res 49:141–154.

Nadol JB, Jr. 1990b. Synaptic morphology of inner and outer hair cells of the human organ of Corti. J Electron Microsc Tech 15: 187–196.

Nadol JB, Jr. 2001. Histopathology of residual and recurrent conductive hearing loss after stapedectomy. Otol Neurotol 22: 162–169.

Nadol JB, Jr., Burgess BJ. 1994. Supranuclear efferent synapses on outer hair cells and Deiters' cells in the human organ of Corti. Hear Res 81:49–56.

Nadol JB, Jr., Eddington DK. 2006. Histopathology of the inner ear relevant to cochlear implantation. Adv Otorhinolaryngol 64: 31–49.

Nadol JB, Jr., Shiao JY, Burgess BJ, Ketten DR, Eddington DK, Gantz BJ, Kos I, Montandon P, Coker NJ, Roland JT, Jr., Shallop JK. 2001. Histopathology of cochlear implants in humans. Ann Otol Rhinol Laryngol 110:883–891.

Nomura Y, Kawabata I. 1979. Loss of stereocilia in the human organ of Corti. Arch Otorhinolaryngol 222:181–185.

Okuno H, Sando I. 1988. Anatomy of the round window. A histopathological study with a Graphic reconstruction method. Acta Otolaryngol 106:55–63.

Osborne MP, Comis SD, Johnson AP, Jeffries DR. 1989. Post-mortem changes in hair bundles of the guinea pig and human cochlea studied by high-resolution scanning microscopy. Acta Otolaryngol 108:217–226.

Ota CS, Kimura RS. 1980. Ultrastructural study of the human spiral ganglion. Acta Otolaryngol 89:53–62.

Pamulova L, Linder B, Rask-Andersen H. 2006. Innervation of the apical turn of the human cochlea: a light microscopic and transmission electron microscopic investigation. Otol Neurotol 27: 270–275.

Proctor B, Bollobas B, Niparko JK. 1986. Anatomy of the round window niche. Ann Otol Rhinol Laryngol 95(5, Pt 1):444–446.

Pujol R, Zajic G, Dulon D, Raphael Y, Altschuler RA, Schacht J. 1991. First appearance and development of motile properties in outer hair cells isolated from guinea-pig cochlea. Hear Res 57: 129–141.

Raphael Y, Altschuler RA. 2003. Structure and innervation of the cochlea. Brain Res Bull 60:397–422. (Review).

Rask-Andersen H, Illing RB. 2004. Human round window membrane receptor. Audiol Med 3:182–192.

Rask-Andersen H, Erixon E, Kinnefors A, Löwenheim H, Schrott-Fischer A, Liu W. 2011. Anatomy of the human cochlea—implications for cochlear implantation. Cochlear Implants Int 12(Suppl 1):S8–S13.

Rask-Andersen H, Kinnefors A, Illing RB. 1999. A novel type of neuron with proposed mechanoreceptor function in the human round window: an immunohistochemical study. Rev Laryngol Otol Rhinol 120:203–207.

Rask-Andersen H, Liu W, Bostrom M, Kinnerfors A. 2010. Immunolocalization of prestin in the human cochlea. Audiol Med 8:56–62.

Rask-Andersen H, Liu W, Linthicum F. 2010. Ganglion cell and 'dendrite' populations in electric acoustic stimulation ears. Adv Otorhinolaryngol 67:14–27.

Rask-Andersen H, Schrott-Fischer A, Pfaller K, Glueckert R. 2006. Perilymph/modiolar communication routes in the human cochlea. Ear Hear 27:457–465.

Rask-Andersen H, Stahle J, Wilbrand H. 1977. Human cochlear aqueduct and its accessory canals. Ann Otol Rhinol Laryngol 86: 1–16.

Rask-Andersen H, Tylstedt S, Kinnerfors A, Illing R. 1997. Synapses on human spiral ganglion cells: a transmission electron microscopy and immunohistochemical study. Hear Res 141:129–39.

Rask-Andersen H, Tylstedt S, Kinnefors A, Schrott-Fischer. 1997. Nerve fiber interaction with large ganglion cells in the human spiral ganglion: a TEM study. Auris Nasus Larynx 24:1–11.

Rattay F, Leao RN, Felix H. 2001a. A model of the electrically excited human cochlear neuron. II. Influence of the three-dimensional cochlear structure on neural excitability. Hear Res 153: 64–79.

Rattay F, Lutter P, Felix H. 2001b. A model of the electrically excited human cochlear neuron. I. Contribution of neural substructures to the generation and propagation of spikes. Hear Res 153:43–63.

Reiss G. 1990. Investigation of intracellular organelles in the human organ of Corti using backscattered electrons (BSE). Acta Otolaryngol Suppl 470:23–27.

Reiss G, Vollrath M. 1990. Scanning electron microscopy in a case of infantile inborn deafness. Acta Otolaryngol Suppl 470:109–113.

Retzius G. 1884. Das gehörorgans der wirbelthiere. II. Das gehörorgan der reptilien, der vögel and der säugethiere. Stockholm: Samson & Wallin.

Rosbe KW, Burgess BJ, Glynn RJ, Nadol JB Jr. 1996. Morphologic evidence for three cell types in the human spiral ganglion. Hear Res 93:120–127.

Scarpa A. 1772. Anatomicae observationes de structura fenestrae rotundae et de tympano secundario. Modena: Typographicam Societatum.

Schrott-Fischer A, Egg G, Kong WJ, Renard N, Eybalin M. 1994. Immunocytochemical detection of choline acetyltransferase in the human organ of Corti. Hear Res 78:149–157.

Schrott-Fischer A, Kammen-Jolly K, Scholtz AW, Glückert R, Eybalin M. 2002a. Patterns of GABA-like immunoreactivity in efferent fibers of the human cochlea. Hear Res 174:75–85.

Schrott-Fischer A, Kammen-Jolly K, Scholtz AW, Kong WJ, Eybalin M. 2002b. Neurotransmission in the human labyrinth. Adv Otorhinolaryngol 59:11–17.

Schuknecht HF, Gacek MR. 1993. Cochlear pathology in presbycusis. Ann Otol Rhinol Laryngol 102:1–16.

Sellers LM. 1961. The round window—a critical re-evaluation. Laryngoscope 71:237–257.

Sellers LM, Anson B. 1962. Anatomical observations on the round window by Antonio Scarpa. Arch Otolaryngol 75:2–45.

Shepherd RK, Coco A, Epp SB, Crook JM. 2005. Chronic depolarization enhances the trophic effects of brain-derived neurotrophic factor in rescuing auditory neurons following a sensorineural hearing loss. J Comp Neurol 486:145–158.

Shepherd RK, Matsushima J, Martin RL, Clark GM. 1994. Cochlear pathology following chronic electrical stimulation of the auditory nerve. II. Deafened kittens. Hear Res 81:150–166.

Slepecky NB, Ulfendahl M. 1992. Actin-binding and microtubule-associated proteins in the organ of Corti. Hear Res 57:201–215.

Slepecky NB, Cefaratti LK, Yoo TJ. 1992a. Type II and type IX collagen form heterotypic fibers in the tectorial membrane of the inner ear. Matrix 12:80–86.

Slepecky NB, Savage JE, Cefaratti LK, Yoo TJ. 1992b. Electron-microscopic localization of type II, IX, and V collagen in the organ of Corti of the gerbil. Cell Tissue Res 267:413–418.

Slepecky NB, Savage JE, Yoo TJ. 1992c. Localization of type II, IX and V collagen in the inner ear. Acta Otolaryngol 112:611–617.

Spicer SS, Schulte BA. 1991. Differentiation of inner ear fibrocytes according to their ion transport related activity. Hear Res 56:53–64.

Spoendlin H. 1971. Primary structural changes in the organ of Corti after acoustic overstimulation. Acta Otolaryngol 71:166–176.

Spoendlin H. 1978. Report of the conference for inner ear biology, Bordeaux 1977 (author's transl). HNO 26:361–365.

Spoendlin H. 1979. Sensory neural organisation of the cochlea. J Laryngol Otol 93:853–877.

Spoendlin H. 1985. Anatomy of cochlear innervation. Am J Otolaryngol 6:453–467.

Spoendlin H, Schrott A. 1988. The spiral ganglion and the innervation of the human organ of Corti. Acta Otolaryngol 105:403–410.

Spoendlin H, Schrott A. 1989. Analysis of human auditory nerve. Neuroscience 43:25–38.

Spoendlin H, Schrott A. 1990. Quantitative evaluation of the human cochlear nerve. Acta Otolaryngol Suppl 470:61–69; discussion 69–70.

Su W, Marion MS, Matz GJ, Hinojosa R. 1982. Anatomical measurements of the cochlear aqueduct, round window membrane, round window niche and facial recess. Laryngoscope 92:483–486.

Takahashi H, Takagi A, Sando I. 1989. Computer-aided three-dimensional reconstruction and measurement of the round window and its membrane. Otolaryngol—Head Neck Surg 101:517–521.

Tanaka K, Sakai N, Terayama Y. 1979. Organ of Corti in the human fetus: scanning and transmission electronmicroscope studies. Ann Otol Rhinol Laryngol 88(Pt 1):749–758.

Thalmann I. 1993. Collagen of accessory structures of organ of Corti. Connect Tissue Res 29:191–201.

Tian Q, Linthicum FH, Jr., Fayad JN. 2006. Human cochleae with three turns: an unreported malformation. Layngoscope 116:800–803.

Toth M, Alpar A, Patonay L, Olah I. 2006. Development and surgical anatomy of the round window niche. Ann Anat 188:93–101.

Tsuprun V, Santi P. 2001. Proteoglycan arrays in the cochlear basement membrane. Hear Res 157:65–76.

Tylstedt S, Rask-Andersen H. 2001. A 3D model of membrane specialization between human auditory spiral ganglion cells. J Neurocytol 30:465–473.

Tylstedt S, Kinnefors A, Rask-Andersen H. 1997. Neural interaction in the human spiral ganglion: a TEM study. Acta Otolaryngol 117:505–512.

Ulehlova L, Voldrich L, Janisch R. 1987. Correlative study of sensory cell density and cochlear length in humans. Hear Res 28:149–151.

Verbist BM, Ferrarini L, Briaire JJ, et al. 2009. Anatomic considerations of cochlear morphology and its implications for insertion trauma in cochlear implant surgery. Otol Neurotol 30:471–477.

Verhoeven K, Van Laer L, Kirschhofer K, Legan PK, Hughes DC, Schatteman I, Verstreken M, Van Hauwe P, Coucke P, Chen A, Smith RJ, Somers T, Offeciers FE, Van de Heyning P, Richardson GP, Wachtler F, Kimberling WJ, Willems PJ, Govaerts PJ, Van Camp G. 1998. Mutations in the human alpha-tectorin gene cause autosomal dominant non-syndromic hearing impairment. Nat Genet 19:60–62.

von Békésy G. 1960. Experiments in hearing. New York: McGraw-Hill. 745 p.

Wadin K. 1988. Radioanatomy of the high jugular fossa and the labyrinthine portion of the facial canal. A radioanatomic and clinical investigation. Acta Radiol Suppl 372:29–52.

Wilbrand HF, Rask-Andersen H, Gilstring D. 1974. The vestibular aqueduct and the para-vestibular canal. An anatomic and roentgenologic investigation. Acta Radiol Diagn (Stockh) 15:337–355.

Wright A. 1980a. Scanning electron microscopy of the human cochlea—the stria vascularis. Arch Otorhinolaryngol 229:39–44.

Wright A. 1984. Dimensions of the cochlear stereocilia in man and the guinea pig. Hear Res. 13:89–98.

Wright A. 1980b. Scanning electron microscopy of the human cochlea—postmortem autolysis artefacts. Arch Otorhinolaryngol 228:1–6.

Wright A. 1981a. Scanning electron microscopy of the normal human cochlea. Clin Otolaryngol Allied Sci 6:237–244.

Wright A. 1981b. Scanning electron microscopy of the human cochlea—the organ of Corti. Arch Otorhinolaryngol 230:11–19.

Wright A. 1982. Giant cilia in the human organ of Corti. Clin Otolaryngol Allied Sci 7:193–199.

Wright A. 1983. Scanning electron microscopy of the human organ of Corti. J R Soc Med 76:269–278.

Wright CG, Preston RE. 1976. Efferent nerve fibers associated with the outermost supporting cells of the organ of Corti in the guinea pig. Acta Otolaryngol 82:41–47.

Wright CG, Schaefer SD. 1982. Inner ear histopathology in patients treated with cis-platinum. Laryngoscope 92:1408–1413.

Wright A, Davis A, Bredberg G, Ulehlova L, Spencer H. 1987. Hair cell distributions in the normal human cochlea. Acta Otolaryngol Suppl 444:1–48.

Wysocki J. 1998. Zmiennosc wejsia do niszy okienaokraglego u dziecii doroslych. Otolaryngol Pol 52:463–466.

Zheng J, Shen W, He DZZ, Long K, Madison LD, Dallos P. 2000. Prestin is the motor protein of cochlear outer hair cells. Nature 405:149–155.